The response of the maize nitrate transport system to nitrogen demand and supply across the lifecycle

Trevor Garnett[1,2*], Vanessa Conn[1,2], Darren Plett[1,2], Simon Conn[1,2], Juergen Zanghellini [1,3], Nenah Mackenzie[1,2], Akiko Enju[1,2], Karen Francis[1,2], Luke Holtham[1,2], Ute Roessner[4,5], Berin Boughton[4,5],Antony Bacic[4,5], Neil Shirley[1,2], Antoni Rafalski[6], Kanwarpal Dhugga[7], Mark Tester[1,2] , Brent N. Kaiser[2]

[1]Australian Centre for Plant Functional Genomics, Waite Research Institute, University of Adelaide, Adelaide, South Australia, 5064, AUSTRALIA

[2]School of Agriculture, Food and Wine, Waite Research Institute, University of Adelaide, Adelaide, South Australia, 5064, AUSTRALIA,

[3]Austrian Centre of Industrial Biotechnology, Vienna, A1190, AUSTRIA

[4]Australian Centre for Plant Functional Genomics, School of Botany, The University of Melbourne, Parkville, Victoria, 3010, AUSTRALIA

[5]Metabolomics Australia, School of Botany, University of Melbourne, Victoria, 3010, AUSTRALIA

[6]DuPont Crop Genetics, Wilmington, Delaware, 19803, USA

[7]Agricultural Biotechnology, DuPont Pioneer, Johnston, Iowa, 50131, USA

Author for correspondence: Trevor Garnett: +61 408408085; trevor.garnett@acpfg.com.au

Total word count:	**6440**
Introduction:	857
Materials and Methods:	1160
Results:	2417
Discussion:	1951
Acknowledgments:	55
Figures:	9
Supporting Information figures:	7
Supporting Information tables:	2

SUMMARY

- An understanding of nitrate (NO_3^-) uptake throughout the lifecycle of plants and how this process responds to N availability is an important step towards the development of plants with improved nitrogen use efficiency.
- NO_3^- uptake capacity and transcript levels of putative high and low affinity NO_3^- transporters were profiled across the lifecycle of dwarf maize (*Zea mays*) plants grown at reduced and adequate NO_3^-.
- Plants showed major changes in high affinity NO_3^- uptake capacity across the lifecycle which varied with changing relative growth rates of roots and shoots. Transcript abundance of putative high affinity NO_3^- transporters (predominantly *ZmNRT2.1* and *ZmNRT2.2*) were correlated with two distinct peaks in high-affinity root NO_3^- uptake capacity and also N availability. Reducing NO_3^- supply during the lifecycle led to a dramatic increase in NO_3^- uptake capacity which preceded changes in transcript levels of NRTs, suggesting a model with short term post-translational regulation and longer term transcriptional regulation of NO_3^- uptake capacity.
- These observations offer new insight into the control of NO_3^- uptake by both plant developmental processes and N availability and identifies key control points that future plant improvement programs may target to enhance N uptake relative to availability and/or demand.

KEYWORDS

maize, nitrogen, nitrate, nitrogen use efficiency, NUE, uptake

INTRODUCTION

A vast amount (>100 million T) of nitrogen (N) fertilisers are applied to crops annually to maximise yield (FAO, 2006). However, in cereal production, only 40-50 % of the applied N is actually taken up by the intended crop (Peoples *et al.*, 1995; Sylvester-Bradley & Kindred, 2009). Given this low N uptake efficiency, we believe a better understanding of the N uptake process in cereals would help identify the limiting factors contributing to poor N uptake efficiency and overall cereal N use efficiency (NUE). NUE in this case refers to grain yield per unit of available N in the soil (Moll *et al.*, 1982; Dhugga & Waines, 1989; Good *et al.*, 2004).

This study is focussed on the uptake and use of NO_3^- as it is the predominant form of N in most high-input agricultural soils (Wolt, 1994; Miller *et al.*, 2007). Plant NO_3^- uptake generally involves two types of transport systems, one involving high-affinity (HATS) and another low-affinity (LATS) transporters (Glass, 2003). In Arabidopsis, four NO_3^- transporters have been linked to NO_3^- uptake from the soil: NRT1.1 and NRT1.2 from the LATS class, and NRT2.1 and NRT2.2 from the HATS (Tsay *et al.*, 2007). NRT 1.1 (Chl1) is unique among these in that it displays dual-affinity towards nitrate depending upon its phosphorylation status (Liu *et al.*, 1999). Although we now have some fundamental knowledge of the functionality of these transporters, our understanding of their roles and of the regulation of NO_3^- uptake remains limited.

Certain aspects of the regulation of the *Arabidopsis* uptake system have been extensively examined. For example, the NO_3^- uptake capacity of the HATS shows strong induction when plants are exposed to NO_3^- after a period of N starvation and uptake capacity is repressed following a period of sufficient NO_3^- (Minotti *et al.*, 1969; Jackson *et al.*, 1973; Goyal &

Huffaker, 1986; Aslam *et al.*, 1993; Henriksen & Spanswick, 1993; Zhuo *et al.*, 1999). This strong induction and repression is reflected in the transcript levels of *AtNRT2.1* and *AtNRT2.2*, which follow the induction and repression of the uptake capacity (Zhuo *et al.*, 1999; Okamoto *et al.*, 2003). Redinbaugh and Campbell (1993) referred to this pattern of induction and repression as the primary NO_3^- response. Whether this N response is relevant to longer time scales and to soil N characteristics of typical cropping soils has yet to be shown.

The relative roles of NRT transporters in the uptake of NO_3^- from the soil remain unclear but circumstantial evidence has been used to postulate their activities. First, the NO_3^- concentration in agricultural soils is generally in the mM range (Wolt, 1994; Miller *et al.*, 2007), well above the point at which the NO_3^- HATS system would be saturated (~ 250 µM) (Siddiqi *et al.*, 1990; Kronzucker *et al.*, 1995; Garnett *et al.*, 2003). Secondly, the location of the transporters within a root suggests variable roles in NO_3^- uptake. *AtNRT1.1* expression is localised in the tips of young roots (Huang *et al.*, 1999; Guo *et al.*, 2001) where roots first come into contact with the higher NO_3^- concentrations of unexplored soil, whereas *AtNRT2.1* is localised in the cortex of older parts of the root where external NO_3^- concentrations may be reduced following uptake at the root tip (Nazoa *et al.*, 2003; Remans *et al.*, 2006). Thirdly, the pattern of *NRT2* repression observed in roots exposed to sufficient N would seem to limit their relative importance to steady-state NO_3^- uptake in N rich soils. Given this evidence it has been proposed that the LATS system is most likely responsible for the majority of NO_3^- uptake from the soil (Glass, 2003).

Little is known of how NO_3^- uptake is actually managed over the lifecycle of the plant with many studies on NO_3^- uptake focussed on responses to perturbations where external NO_3^- availability is varied in order to explore NO_3^--dependent uptake responses. In one of the few

published studies, Malagoli et al. (2004) measured the uptake capacity of the NO_3^- HATS and LATS in oilseed rape over time and their response to various factors and used this information, together with modelling of field data, to suggest that the NO_3^- HATS could supply most of the plants N requirements, even with high N availability. This work suggests the HATS is important in net NO_3^- uptake, necessitating a re-examination of the respective roles of these two transport systems. A detailed analysis of NO_3^- uptake capacity across the entire lifecycle is an important step towards the development of plants with enhanced N uptake capacity and efficiency, and may help improve N fertilisation practise where supply can be better matched to demand.

In this study, we have profiled changes in NO_3^- uptake capacity in maize plants across a broad developmental time period in response to either reduced or adequate NO_3^- provision. During the lifecycle, the plants were changed between NO_3^- treatments to help distinguish between developmental changes. Given the problems inherent in using a full-sized maize plant for such experiments, we have used the dwarf maize 'Gaspe Flint,' which has a lifecycle of just 60 days, allowing profiling across both vegetative and reproductive stages in a contained environment (Hourcade *et al.*, 1986).

MATERIALS AND METHODS

Plant Growth

Seeds of the dwarf maize (*Zea mays* var. Gaspe Flint) were germinated on moist filter paper for 4 d at 28°C. Seedlings were transferred to 1 of 2 700 l ebb and flow hydroponic systems with the fill/drain cycles completed in 13 min. Initially 150 plants were planted in each system. Plants were grown on mesh collars within tubes (300 mm x 50 mm) which kept roots

of adjacent plants separate but allowed free access to solution. The hydroponic system was situated in a controlled environment room with 14/10-h 25°C/20°C day/night cycle at a flux density at canopy level of approximately 500 µmol m^{-2} s^{-1}. The nutrient solution was a modified Johnson's solution (Johnson *et al.*, 1957) containing either (in mM) 0.5 NO_3-N, 0.8 K, 0.1 Ca, 0.5 Mg, 1 S, and 0.5 P for the 0.5 mM NO_3^- treatment or (in mM): 2.5 NO_3-N, 1.8 K, 0.6 Ca, 0.5 Mg, 0.5 S, and 0.5 P for the 2.5 mM NO_3^- treatment. The choice of concentration was based on preliminary experiments which suggested that the threshold NO_3^- concentration eliciting a major N response would be approximately 0.5 mM and this would appear to be the case (Supporting information Fig. S1). Both treatment solutions contained (in µM): 2 Mn, 2 Zn, 25 B, 0.5 Cu, 0.5 Mo, 100 Fe (as FeEDTA and FeEDDHA). Iron was supplemented twice weekly with the addition of $Fe(NH_4)_2(SO_4)_2.6H_2O$ (8 mg l^{-1}). Solution pH was maintained between 5.9 and 6.1. NO_3^- was monitored using a NO_3^- electrode (TPS, Springwood, Australia) and maintained at the target concentration ± 10%. Other nutrients were monitored using an inductively coupled plasma optical emission spectrometer (ICP-OES: ARL 3580 B, ARL, Lausanne, Switzerland) and showed limited depletion between solution changes. Nutrient solutions were changed every 20 days.

Flux measurement

On sampling days, between 1100 and 1300 h, plants were transferred to a controlled environment room with conditions matching growth conditions (light, temperature and relative humidity) and into solutions matching growth solutions. The roots were then given a 5-minute rinse with the same nutrient solution but with either 50 or 250 µM NO_3^-, followed by 10 minute exposure to the same solution but with ^{15}N labelled NO_3^- (^{15}N 10%). In preliminary experiments, flux measured at 50 and 250 µM NO_3^- was found to be before (50 µM) and at the point of saturation (250 µM) of the HATS uptake system. At the end of the

flux period roots were rinsed for 2 minutes in matching but unlabelled solution. Two identical solutions were used for this rinse to allow an initial 5 second rinse to remove labelled solution adhering to the root surface. The flux timing was based on that used by Kronzucker *et. al* (1995) and chosen to minimise any possible efflux or transport to the shoot.

Roots were blotted, and then roots and separated shoots weighed and then dried at 65°C for 7 days after which the roots were ground to a fine powder (Clarkson *et al.*, 1996). Total N and ^{15}N in the plant samples were determined with an isotope ratio mass spectrometer (Sercon, Cheshire, UK). Unidirectional NO_3^- influx was calculated based on ^{15}N content of the root. The unidirectional NO_3^- influx measured in this study is described as the uptake capacity of the plant at that point in the lifecycle.

Quantitative real time PCR

On sampling days root material was harvested between 5 and 7 hours after the start of the light period. The whole root was excised and snap-frozen in liquid nitrogen and stored at -80°C. RNA was extracted using the RNeasy Plant Mini Kit with on-column DNase treatment (Qiagen, Hilden, Germany) according to the manufacturer's instructions before RNA integrity was checked on a 1.2% (w/v) agarose gel. cDNA synthesis was performed on 1 µg of total RNA with oligo$(dT)_{19}$ using SuperScript III reverse transcriptase (Invitrogen, Carlsbad, CA, USA) according to the manufacturer's instructions. Real-time quantitative PCR (Q-PCR) was carried out as outlined in Burton *et al.* (2008). In this method, the amount of each amplicon in each cDNA is quantified with respect to a standard curve of the expected amplicon (typically, PCR efficiencies ranged between 0.85 and 1.05). Four control genes (*ZmGaPDh, ZmActin, ZmTubulin* and *ZmElF1*) were utilised for the calculation of the normalisation factor. Q-PCR normalisation was carried out as detailed in Vandesompele *et al.* (2002) and Burton *et al*. (2004). Q-PCR primers were designed for the closest maize

169 homologues of the Arabidopsis NRT transporters (Plett *et al.*, 2010). Q-PCR products were
170 verified by sequencing, agarose gel electrophoresis and melt-curve analysis to confirm a
171 single PCR product was being amplified. All primer sequences and Q-PCR product
172 information for control genes and NRT transporter genes can be found in Supporting
173 Information Table S1.

174 **Nitrate determination**

175 Tissue NO_3^- content was determined via a previous method (Braun-SysteMatic,
176 Methodenblatt N 60; (Rayment & Higginson, 1992)) scaled appropriately for assay in 96-
177 well optical plates. Frozen and ground tissue (100 mg) was aliquoted into 1.1 ml strip tubes
178 in a 96-well format. 600 µl of extraction buffer was added to each tube and the rack of tubes
179 was shaken vigorously for 15 min in a cold room at 4 °C. Extraction buffer was comprised of
180 50 mM HEPES (pH 7.5), 20% (v/v) glycerol, 1 mM EDTA, 1 mM EGTA, 0.1% (v/v) Triton
181 X-100, 1 mM benzamidine, and 1 mM 6-aminohexanoic acid. Racks were centrifuged at
182 3400 *g* at 4°C for 45 min and supernatant was transferred to fresh tubes. Racks were
183 centrifuged at 3400 *g* for an additional 45 min at 4°C and supernatant was transferred to 96-
184 well PCR plates. A clarified soluble extract (15 µl + 10 µl dH_2O) was added to optical plates
185 and 15 µl of freshly prepared 2 mM $CuSO_4$ and 10 µl of 0.2 M hydrazine sulphate were
186 added to each well. Plates were incubated for 5 min at 37°C and 15 µl of 1 M NaOH was
187 added to each well. Plates were shaken and incubated for 10 min at 37°C. A solution (100 µl)
188 containing equal parts 2.5% (w/v) sulphanilamide in 3.75 M HCl and 0.5 % (w/v) N-
189 ethylenediamine was added to each well and plates were incubated at room temperature for
190 10 min. Absorbance was measured at 540 nm. 15 µl of KNO_3 standards (0 –75 nmol/15 µM)
191 were run on each plate and were processed the same as the samples above. Nitrate content
192 was expressed as nmol of NO_3^- per mg of tissue FW.

Amino acid determination

Tissue amino acid concentration was determined using liquid chromatography electrospray ionization-mass spectrometry as described by Broughton *et al.* (2011) once the samples had been derivatised following the method of Cohen and Michaud (1993).

Statistical analyses

Statistical analysis of biomass, flux and metabolite data was carried out using two-way analysis of variance (ANOVA). Data followed a normal distribution. Means of grain yield were tested for significance using a two-tailed t-test. The time course was repeated twice (flux analysis and transcript levels) with similar results.

RESULTS

Biomass

As expected, under our steady-state hydroponic conditions, we observed no difference in either total root or shoot biomass when plants were grown in nutrient solution containing either reduced (0.5 mM) or adequate (2.5 mM) concentrations of NO_3^- (Fig. 1a,b, respectively). With both NO_3^- treatments, there was a considerable drop in the root to shoot ratio over the first 18 days after emergence (DAE), highlighting the rapid shoot growth of the plants in the early vegetative period (Figure 1c). However, our treatments did impact upon the N content between 0.5 and 2.5 mM grown plants (Fig. 1d). Shoot N concentration was significantly greater ($p<0.001$) in the whole shoots of plants grown at 2.5 mM NO_3^- than that of 0.5 mM plants but in both treatments the N concentration was above the critical concentration in the youngest fully expanded blade which is around 2 mmol g DW^{-1} N (Reuter & Robinson, 1997). Based on in-season monitoring, these concentrations reflect

agronomically realistic NO_3^- concentrations (Miller et al., 2007) and for the 0.5 mM treatment represents reduced but not growth impacting NO_3^- levels, which is important in the context of this study. Irrespective of the NO_3^- concentration supplied; there was a continual drop in tissue N across the lifecycle (Fig. 1d). There was no significant difference in final grain yields (grain DW (g), mean ± SEM: 0.5 mM, 1.85 ± 0.38 (n=12); 2.5 mM, 1.80 ± 0.24 (n=8)). The plants at each of the growth stages can be seen in Supporting Information Fig. S2.

Nitrate flux capacity

Unidirectional NO_3^- HATS flux (e.g. high-affinity NO_3^- uptake capacity) into the root at both 50 and 250 µM external concentrations was determined across various stages of the lifecycle of both 0.5 mM and 2.5 mM grown plants (Siddiqi *et al.*, 1990; Kronzucker *et al.*, 1995; Garnett *et al.*, 2003). We observed large but parallel fluctuations in HATS NO_3^- uptake capacity over time at both NO_3^- concentrations (Fig. 2a,b), where NO_3^- uptake capacity peaked twice, one coinciding with early vegetative growth (15 DAE) and the other just prior to flowering (26 DAE). The reduction in uptake capacity between these two peaks (22 DAE) was considerable when measured at 50 µM (~ 20% of the peak value). Aside from the two peaks and the intervening drop, NO_3^- uptake capacity decreased continually from 15 DAE.

HATS uptake capacity of the 0.5 mM NO_3^- grown plants across most of the life cycle was generally higher than the 2.5 mM grown plants (~50% at 50 µM and ~40% at 250 µM). This was particularly evident during the early vegetative period of growth (up to 18 DAE) where NO_3^- uptake capacity measured in 50 µM was significantly enhanced in the plants grown at low external NO_3^- concentrations (Fig. 2a). However, when averaged across the life cycle,

the NO_3^- fluxes measured at 250 µM were approximately 20% higher than those measured at 50 µM.

Nitrogen uptake

To better understand the relationship between growth and N uptake, shoot and root growth, together with tissue N was used to calculate N uptake over the lifecycle. As there was no difference between treatments for root or shoot biomass, the data were pooled for model fitting irrespective of the treatments. The initial shoot growth rate was much higher than the root growth rate and a modified exponential function was required to describe the apparent change in the shoot growth rate early after germination whilst the root data was accurately fitted with an exponential function (Fig. 1, Supporting information Fig. S3). Both functions accurately fit the data with coefficients of determination (R^2) of 0.988 and 0.992 for root and shoot, respectively (Supporting Information Tab. S2). To model the N content, an allometric relation between N content and shoot biomass (Lemaire & Salette, 1984) was fitted (Supporting information Fig. S3 inset). To avoid division by zero, $N = \alpha / (\gamma + DW_S^{\beta})$ was used as a fitting function rather than the usual power law. Here N denotes shoot N, DW_S is shoot dry weight and α, β, γ are fitting parameters, listed in Supporting Information Tab. S2. As a result, an improvement was seen in the goodness of fit from $R^2 = 0.996$ to $R^2 = 0.999$. Root N concentration was constant throughout the lifecycle.

Shoot and root dry weight (DW(t)), and N content, N(DW), were used to calculate the net N uptake of the plants ($N_{tot}(t) = N_S \cdot DW_S(t) + N_R \cdot DW_R(t)$). The N uptake per gDW_R as a function of time (t) is illustrated in Fig. 3 (lines without symbols) and compared with the experimentally determined NO_3^- uptake capacity for both treatments (open and filled squares). All four data sets show a comparable peak around day 15. The experimentally

260 measured second peak around day 26 is less pronounced in the calculated values where a
261 plateau rather than a peak structure is visible. Both features can be understood in terms of the
262 initial mismatch between root and shoot growth rate.

263 Up until 12 DAE, shoots grew almost 6 times faster than roots (Fig. 1a, b, Supporting
264 information Fig. S3). During this time nitrogen concentration in the shoots remained
265 approximately constant at 3.9 mmol g DW^{-1}. It would appear the elevation in N uptake
266 capacity observed by the roots (Fig. 2, 3) is a response to meet plant demand for N. Between
267 10 and 20 DAE, the overall shoot growth rate drops by more than 75% reaching a final value
268 of 0.0032 hr^{-1}. The reduction in shoot growth reduces overall plant demand for N, which is
269 correlated with the observed decrease in measured NO_3^- uptake capacity beginning from 13
270 DAE. Similarly for the second peak (Fig. 2), the exponential phase of shoot growth during
271 this period is roughly 1.3 times faster than that of root growth. Again, it would appear there is
272 a mismatch in growth-dependent N demand relative to N availability requiring an up-
273 regulation of N import mechanisms (Fig. 3, see also Supporting information Fig. S3).
274 However, up-regulation is reduced relative to that of the first peak (Fig. 3). During this
275 period, N concentrations in the shoot decreases from 3.9 mmol gDW^{-1} at 15 DAE to 2.5
276 mmol gDW^{-1} at 40 DAE.

277 The NO_3^- HATS uptake capacity in the 0.5 mM grown plants was remarkably similar to the
278 net N uptake rate as calculated from plant N content (Fig. 3), suggesting there was little
279 overall LATS input. However, in the 2.5 mM treatment the uptake capacity of the HATS was
280 approximately 50% of the actual uptake rate and, given the NO_3^- concentration of this
281 treatment, this suggests there is significant LATS contribution to the net NO_3^- uptake under
282 these conditions. This is supported by our data from experiments in which LATS capacity

was measured at 1 mM and 4 mM and was found to be 30% and 100% of the HATS uptake capacity (0-20 DAE), respectively (Supporting information Fig. S4). This indicates that LATS uptake capacity measured at 2.5 mM would be close to our estimation of 50%.

To further distinguish between developmental and nitrogen responses, a subset of plants were subjected to a change in NO_3^- concentration. At day 15, plants were moved from 0.5 mM to 2.5 mM NO_3^- (*N-inc*) and likewise plants moved from 2.5 mM to 0.5 mM (*N-red*), a process repeated also at day 22. When NO_3^- flux capacity was first measured, 3 days after changing NO_3^- concentrations, at both day 15 and day 22, *N-red* treatments, led to a substantial increase in NO_3^- flux capacity (Fig. 4). In *N-red* treatments at day 15, the initial doubling in uptake capacity relative to plants maintained at 2.5 mM NO_3^- was nonetheless followed by the reduction in uptake capacity at day 22 observed in plants with constant NO_3^- concentration. Following the day 22 dip, the uptake capacity returned to a level higher than those plants kept at 2.5 mM NO_3^-. *N-red* treatments at day 22 showed a dramatic increase in uptake capacity at day 25. *N-inc* treatments (plants moved from 0.5 mM to 2.5 mM NO_3^-) had approximately half the uptake capacity of plants kept at 0.5 mM and this was maintained till day 40 (Fig. 4).

Developmental and nutritional changes to NRTtranscript levels

The recent completion of the maize genome sequence provided the opportunity to complete a rigorous survey of cereal homologues to the Arabidopsis *NRT* genes (Plett *et al.*, 2010), and the naming conventions put forward in that paper are used here. There are currently four *NRT* genes thought to be involved in root NO_3^- uptake in Arabidopsis (Tsay et al., 2007). However, given the dichotomy between the Arabidopsis *NRTs* and the cereal *NRT*s identified by Plett et al. (2010), it was decided to quantify the developmental expression pattern for the

306 relevant maize *NRT1*, *NRT2* and *NRT3(NAR2)* orthologues of all the known Arabidopsis
307 *NRTs* on plants grown at either 0.5 or 2.5 mM NO_3^-.

308 At the whole root level, transcript levels of the putative HATS genes *ZmNRT2.1* and
309 *ZmNRT2.2* were significantly more represented in the total RNA pool than those of the other
310 *NRT2* or *NRT1* genes examined (Fig. 5, Supporting information Fig. S5). This may represent
311 either simple differences in RNA and/or protein stability between the classes of transport
312 proteins but may instead reflect defined roles with respect to NO_3^- transport (Fig. 4). This
313 latter point is suggested by the expression pattern of *ZmNRT2.1* and *ZmNRT2.2* across the
314 lifecycle where transcript responses showed remarkable similarity to the patterns observed in
315 the uptake measurements (Fig. 5, see also Fig. 2 and 3). Interestingly, both *ZmNRT2.1* and
316 *ZmNRT2.2* transcript levels were found to be higher in the roots of plants grown at 0.5 mM
317 NO_3^- than those grown at 2.5 mM, indicating a N-dependent response; this contrasts with
318 most other *NRT* genes where differences in N availability had less of an impact.
319 Notwithstanding the variation in transcript levels of *ZmNRT2.1* and *ZmNRT2.2* across the
320 lifecycle and the N treatments, the baseline transcript levels from which they varied were also
321 very high, being 200 to 300-fold higher than the other NRT2 or NRT1 transporters
322 (*ZmNRT1.1B*) (Fig. 5). Across the lifecycle this baseline showed a reduction for both
323 transporters but was far more pronounced for *ZmNRT2.1*. As regards the other NRT2s,
324 *ZmNRT2.3* showed much lower transcript levels and although there were similar fluctuations
325 across the lifecycle there were no clear differences between N treatments. *ZmNRT2.5*
326 expression was only detectable in the plants grown in the reduced NO_3^- treatment, with
327 significant variation across the lifecycle.

Transcript levels of *ZmNRT1.1A*, *ZmNRT1.1B* and *ZmNRT1.2* were a thousand-fold less than *ZmNRT2.1* and *ZmNRT2.2* and did not show the same pattern of variation over the lifecycle as the *ZmNRT2s* (Fig. 5). Both *ZmNRT1.1A* and *ZmNRT1.1B* showed a peak commencing at 13 DAE coinciding with the *ZmNRT2* peak. *ZmNRT1.2* showed very low transcript levels until 34 DAE from where these increased 10-fold. Apart from *ZmNRT1.5A*, there were no consistent differences in transcript levels of the *NRT1s* that corresponded to treatment differences in either growth or uptake capacity. *ZmNRT1.5A* transcript levels were higher in 0.5 mM NO_3^- plants and had a profile matching that of *ZmNRT2.1* and *ZmNRT2.2*. Transcript levels of *ZmNRT1.1D, ZmNRT1.3, ZmNRT1.4A, ZmNRT1.4B and ZmNRT1.5B* were all very low (Supporting Information Fig. S5), while *ZmNRT1.1C* was undetectable.

The transcript levels of *ZmNRT3.1A* were 20 to 100-fold lower than for *ZmNRT2.1* and *ZmNRT2.2* respectively, but showed the same increase in transcript abundance at 18 and 28 DAE (Fig. 5e). *ZmNRT3.1A* differs in that it also has a third large peak just before 40 DAE. This third peak showed little difference between the two NO_3^- treatments. The profile of *ZmNRT3.2* was more similar to those of *ZmNRT2.1/2.2* but levels were much lower and there were no treatment differences. Transcript levels of *ZmNRT3.1B* were very low (Supporting Information Fig. S5).

As was seen with plants maintained at constant concentrations, when plants were swapped between NO_3^- treatments at days 15 and 22 the genes that showed greatest response to nitrogen were *ZmNRT2.1*, *ZmNRT2.2*, *ZmNRT2.5,* and *ZmNRT1.5a* (Fig. 6, Supporting information Fig. S6). Patterns of response for *ZmNRT2.1*, *ZmNRT2.2* were very similar with plants with increased NO_3^- (*N-inc*) having lower transcript levels than plants with decreased NO_3^- rate concentration (*N-red*).

The transcript profiles of these N responsive genes was interesting in that, immediately after transfer to reduced NO_3^- , transcript levels continued on with the same trend as with before the change in NO_3^-, i.e. they kept decreasing, whilst at the same time there was a doubling in uptake capacity (Fig. 4b and 6). In contrast, *ZmNRT2.1*, *ZmNRT2.2*, *ZmNRT2.5*, and *ZmNRT1.5A* all showed a peak in transcript at day 25, a peak only previously seen in *ZmNRT2.5*. The transcript levels for *ZmNRT2.5* were the most N-responsive with plants moved to higher NO_3^- (*N-inc*) having no measurable transcripts whilst those decreased (*N-red*) having similar peaks to those plants maintained at 0.5 mM NO_3^-. *ZmNRT1.5A*, the only N responsive *ZmNRT1* again showed a major peak in transcript levels at day 25 but none at day 29.

Tissue Nitrate

Leaf NO_3^- concentrations differed between NO_3^- treatments ($p<0.01$). In general, leaves of 2.5 mM treated plants had higher concentrations of NO_3^-. At most time points the trend in NO_3^- concentration was mirrored between the two treatments with the exception where leaf NO_3^- in the 0.5 mM treatment was higher than the 2.5 mM treatment at 29 and 34 DAE. For both treatments leaf NO_3^- concentrations prior to anthesis remained high but then dropped dramatically after 28 DAE (Fig. 7). There was a more consistent trend in root NO_3^- with 2.5 mM treated roots often having higher levels than those exposed to 0.5 mM NO_3^-. Over time, the root trends was similar between treatments in that at 20 DAE there was a doubling of root NO_3^- in both treatments and by 29 DAE both treatments showed a major drop in root NO_3^-. In the 0.5 mM grown plants there was a major spike in root NO_3^- at day 39, a peak also seen in leaf NO_3^-(Fig. 7).

373 **Amino acids**

374 The free amino acid levels showed similar trends in the two NO_3^- treatments (Fig. 8). Apart
375 from the first measurement, where free amino acids in the shoots were very low, root amino
376 acid levels were consistently lower than shoot levels and this difference became greater after
377 day 30 when shoot level increased but root levels remained the same. For the roots, there was
378 an initial decrease followed by a peak at 20 DAE, which was common to both treatments. In
379 the shoots, the patterns are less consistent between treatments, with fluctuations showing little
380 correlation.

381 **DISCUSSION**

382 Across the lifecycle of Gaspe Flint, NO_3^- uptake capacity changed approximately 10-fold
383 irrespective of external N availability. This change was characterised with distinct peaks and
384 troughs in NO_3^- uptake capacity, with a general trend towards decreased NO_3^- uptake capacity
385 as plants grew to maturity, but which were correlated with plant N demand (Fig. 2 and 3).
386 There is also clear evidence that NO_3^- uptake responded positively to reduced N supply, with
387 increased NO_3^- uptake capacity in the lower N treatment (Fig. 2). The transcript profiles of
388 the NO_3^- transporters suggest that changes in uptake capacity, in response to NO_3^- supply and
389 demand, are linked to changes in expression of the putative high affinity NO_3^- transporters
390 *ZmNRT2.1* and *ZmNRT2.2*. Their expression profiles, in response to N supply and time,
391 provide strong correlative evidence of their *in planta* roles in NO_3^- uptake. When N supply
392 was varied (*N-inc* or *N-red*) the commonality in change to *ZmNRT2.1* and *ZmNRT2.2*
393 transcript levels and associated change in NO_3^- flux capacity further support this role. We
394 believe the highly dynamic nature of N acquisition displayed here and the strong relationship

395 to N provision provides a new insight into the regulation of NO_3^- uptake that may lead to the
396 manipulation of N uptake efficiency and ultimately NUE in plants.

397 **Nitrate uptake capacity responding to demand**

398 The NO_3^- uptake capacity was extremely variable across the lifecycle. It has long been
399 suggested that growth rate determines N uptake rate (Clement *et al.*, 1978; Lemaire &
400 Salette, 1984; Clarkson *et al.*, 1986). Data presented here supports this hypothesis; where the
401 relative differences in growth rates between shoots and roots lead to variability in N demand
402 and changes in NO_3^- uptake capacity (Fig. 1 and 3). In both treatments we showed that NO_3^-
403 uptake capacity increased with peaks in shoot growth and consequently N demand but also
404 decreased rapidly when shoot growth decreased creating a characteristic trough in NO_3^-
405 uptake capacity (Fig. 1 and 3). We propose that during this period, the plants grown in 0.5
406 mM NO_3^- were responding to N-limitation and it was plasticity in NO_3^- uptake capacity
407 (HATS) that allowed sufficient N uptake to match the growth rate of the plants grown in 2.5
408 mM NO_3^-. This plasticity is highlighted by the rapid changes in NO_3^- uptake capacity
409 observed in plants that were changed between NO_3^- treatments.

410 The manner in which NO_3^- uptake capacity changes in plants with a sustained reduction in
411 availability of N remains unclear. Most of the literature presents responses in uptake capacity
412 when N is resupplied to plants after a period of reduced N availability and normally resulting
413 in a transient increase in measured NO_3^- uptake capacity (Lee, 1982; Lee & Drew, 1986; Lee
414 & Rudge, 1986; Morgan & Jackson, 1988; Siddiqi *et al.*, 1989). Indeed, there are few results
415 in the literature with which to compare these lifecycle variations in uptake capacity. The
416 work of Malagoli et al. (2004) with oilseed rape is closest in terms of measuring uptake
417 capacity over the lifecycle. Similar to this study, a spike in NO_3^- uptake capacity was

observed corresponding to the time of flowering, however earlier changes in NO_3^- flux capacity (as observed in the study) were not measured.

Transcript levels of the *ZmNRTs*

The measurement of unidirectional NO_3^- influx at 50 and 250 µM was chosen to describe the uptake capacity of the NO_3^- HATS. Based on reliable estimates from the literature the NO_3^- HATS for most plants is saturated at approximately 250 µM (Siddiqi *et al.*, 1990; Kronzucker *et al.*, 1995; Garnett *et al.*, 2003). Given the relatively high NO_3^- concentrations, at least in the 2.5 mM treatment, which were well above the point at which the HATS would be saturated, it was anticipated that the LATS would be responsible for much of the uptake. We also expected there would be little variability in the HATS activity based on the steady-state conditions in which we grew the plants, where constitutive (cHATS) activity would be predicted to dominate, and iHATS being repressed after continued exposure to NO_3^-. However, this was not the case in either treatment as evidenced in the influx analysis described above, and in the expression patterns of the NRT gene families, where the NO_3^- HATS responds intimately to NO_3^- supply and demand.

Previous evidence has suggested HATS transcript levels are generally negatively regulated when N levels are high (e.g. 0.5 to 2.5 mM NO_3^-) (Filleur *et al.*, 2001; Okamoto *et al.*, 2003; Santi *et al.*, 2003; Okamoto *et al.*, 2006; Liu *et al.*, 2009). However in this study we found the opposite, where the baseline transcript levels of *ZmNRT2.1* and *ZmNRT2.2* were generally much higher than for any of the other transporters regardless of external N supply. Following the paradigm suggested by Glass (2003), the role of the HATS system is to acquire NO_3^- only when soil solution concentrations are low, well below the consistent 0.5 mM or 2.5 mM

levels used here. However, the high abundance of *ZmNRT2.1* and *ZmNRT2.2* transcripts, independent of external N supply suggests alternate roles for these gene products.

The high level of transcripts of the two putative HATS transporters (*ZmNRT2.1* and *ZmNRT2.2*) contrasts with the low transcript levels observed for the putative NO_3^- LATS transporters, the *ZmNRT1s,* across the life cycle. Despite differences in the abundance of LATS and HATS transcripts, there were some parallels in the expression patterns particularly during the initial peak in NO_3^- uptake capacity (Fig. 5, Supporting information Fig. S5). These data support previous reports (Ho *et al.*, 2009) of a possible link between NRT1 and NRT2 transport systems, although in maize the relationship may only extend to the early vegetative stage where NO_3^- uptake capacity is at its maximum. Although the transcript levels of *ZmNRT2.5* were very low, the observation that transcripts were only detected in the reduced NO_3^- treatment suggests this putative transporter may play an important role in low N responses.

The delivery of NO_3^- into the xylem in Arabidopsis has been suggested to involve the NO_3^- transporter AtNRT1.5 (Lin et al 2008). Unlike other *ZmNRT1* genes, *ZmNRT1.5A* showed a similar transcript profile to *ZmNRT2.1/2.2* and was responsive to the 0.5 mM treatment, this being consistent with a possible role in loading NO_3^- into the xylem in maize.

The transcript levels of *ZmNRT3.1A* were closest in terms of absolute levels to *ZmNRT2.1 /2.2.* There is good evidence that AtNRT3.1 is essential to the function of the AtNRT2s (Okamoto *et al.*, 2006; Orsel *et al.*, 2006; Wirth *et al.*, 2007). Based on transcript levels and the similarity in pattern across the lifecycle, this would seem also to be true for the maize homologues.

The regulation of nitrate uptake capacity

There is a correlation between the NO_3^- uptake capacity of the HATS and the transcript levels of both *ZmNRT2.1* and *ZmNRT2.2*. This has been found in plants other than maize and has been proposed as evidence of the involvement of the *NRT2s* in NO_3^- uptake (Forde & Clarkson, 1999; Lejay *et al.*, 1999; Zhuo *et al.*, 1999; Okamoto *et al.*, 2003). Combined with the impairment of NO_3^- uptake associated with reduced transcript levels in Arabidopsis *AtNRT2.1* and *AtNRT2.2* knockout mutants (Filleur et al., 2001), this led to the proposal that uptake via *AtNRT2.1* and *AtNRT2.2* is regulated at the transcriptional level. However, transcript levels may not equate to levels of functional protein. Wirth et al. (2007) suggest that the NRT2s in Arabidopsis are long-lived proteins and have shown that the level of AtNRT2.1 protein was independent of transcript level or changes in uptake capacity, suggesting there is considerable post-translational control of NRT2 mediated NO_3^- uptake.

The results presented here are compatible with a model that combines both transcriptional and post-translational control of NO_3^- uptake capacity (Fig 9). In this model the total concentration of ZmNRT2.1 and ZmNRT2.2 protein is predicted as being proportional to the sum of the *ZmNRT2.1* and *ZmNRT2.2* transcript levels at any given day plus, based on an estimated protein lifespan of NRT2 proteins to be ~ 5 days (Wirth et al. (2007), the sum of the transcript levels for the previous 4 days. This 5 day lifespan is based on Wirth *et al.* (2007), but estimates with a range of lifespans are shown in Supporting information Fig. S7. This estimated protein concentration represents the maximal uptake capacity of NRT2.1 and 2.2 at a given day, the actual uptake capacity being dependent on the amount of post-translational inhibition, which could be through allosteric inhibition, phosphorylation, or, given the results of Yong et al. (2010), perhaps due to NRT2/NRT3(NAR2) complexes being removed from the plasma membrane.

As presented in Figure 9, this model predicts that, up until day 15, the NO_3^- uptake capacity was equal to the potential uptake capacity, after which the actual uptake capacity as measured then reduced and became less than the potential uptake capacity. At day 22 the measured uptake capacity increased through the utilisation of the potential uptake capacity without a transcriptional response. This changed at day 27 where, based on our model, the NRT2 protein levels were not enough to provide the required uptake capacity, this leading to the transcriptional peak observed at day 29. In terms of the plants moved from 2.5 mM to 0.5 mM NO_3^- at day 15, the initial increase in uptake capacity seen at day 18 in Figure 4b (and Fig 9b) would be due to a release of post-translational inhibition, hence the increased uptake capacity without a comparable increase in transcript levels (Fig. 6). The peak in *NRT2.1* transcript levels at day 25 would be due to the number of NRT2.1 proteins, in these plants previously exposed to a much higher NO_3^- concentration, not providing enough uptake capacity even with no post-translational inhibition. This model would have transcription providing long term regulation of NO_3^- uptake capacity with short term uptake capacity regulated via post-translational regulation of the existing transport capacity, this short term regulation being important for N homeostasis.

The current model of the regulation of NO_3^- uptake by the plant N status (tissue concentrations of NO_3^- itself or a downstream assimilate such as amino acids) which has been described in numerous reviews (Cooper & Clarkson, 1989; Imsande & Touraine, 1994; Forde, 2002; Miller *et al.*, 2008; Gojon *et al.*, 2009). The two component model of NO_3^- uptake capacity regulation described above requires two triggers in its regulation, one a transcriptional trigger and another that determines the extent of post translational inhibition. Given the major drop in transcript levels beginning at day 18 until day 22, it may be that the trigger for the transcriptional response is the root amino acid/ NO_3^- levels which increase and

come to a peak at day 22 (Fig. 7 and 8). The decrease in uptake capacity beginning at day 15, which we propose is due to an increase in post-translation inhibition, could be triggered by shoot amino acid/ NO_3^- levels which peak at this point.

NUE increased through increased uptake capacity with reduced N availability

The results provide clear evidence that NO_3^- uptake capacity in maize changes dynamically across the developmental growth cycle in maize in response to changes in demand. As previously suggested (Filleur *et al.*, 2001; Okamoto *et al.*, 2003; Santi *et al.*, 2003; Okamoto *et al.*, 2006; Liu *et al.*, 2009), NO_3^- uptake capacity is highly responsive to N availability and that *NRT2.1* and *NRT2.2* transcription is most-likely linked to this response. The focus of future work will be an analysis of NRT protein levels, global gene expression and metabolite concentrations at key points of the lifecycle with the aim of gaining a better understanding of how NO_3^- transport is regulated. Such knowledge may benefit programs directed at increasing NUE, and more specifically N uptake efficiency, in maize.

ACKNOWLEDGEMENTS

The authors gratefully acknowledge the technical assistance of Stephanie Feakin and Jaskaranbir Kaur, and Steve Tyerman for a critical reading of the manuscript. This project was funded by the Australian Centre for Plant Functional Genomics, DuPont Pioneer, Australian Research Council Linkage Grant (LP0776635) to B.N.K., M.T. (University of Adelaide) A.R. and K.D. (DuPont Pioneer).

LITERATURE CITED

Aslam M, Travis RL, Huffaker RC. 1993. Comparative induction of nitrate and nitrite uptake and reduction systems by ambient nitrate and nitrite in intact roots of barley (*Hordeum vulgare* L) seedlings. *Plant Physiology* **102**: 811-819.

Boughton BA, Callahan DL, Silva C, Bowne J, Nahid A, Rupasinghe T, Tull DL, McConville MJ, Bacic A, Roessner U. 2011. Comprehensive Profiling and Quantitation of Amine Group Containing Metabolites. *Analytical Chemistry* **83**: 7523-7530.

Burton RA, Jobling SA, Harvey AJ, Shirley NJ, Mather DE, Bacic A, Fincher GB. 2008. The genetics and transcriptional profiles of the cellulose synthase-like HvCslF gene family in barley. *Plant Physiology* **146**: 1821-1833.

Burton RA, Shirley NJ, King BJ, Harvey AJ, Fincher GB. 2004. The CesA gene family of barley. Quantitative analysis of transcripts reveals two groups of co-expressed genes. *Plant Physiology* **134**: 224-236.

Clarkson DT, Gojon A, Saker LR, Wiersema PK, Purves JV, Tillard P, Arnold GM, Paans AJM, Vaalburg W, Stulen I. 1996. Nitrate and ammonium influxes in soybean (*Glycine max*) roots -direct comparison of N-13 and N-15 tracing. *Plant Cell and Environment* **19**: 859-868.

Clarkson DT, Hopper MJ, Jones LHP. 1986. The effect of root temperature on the uptake of nitrogen and the relative size of the root system in *Lolium perenne.* I. Solutions containing both NH_4^+ and NO_3^-. *Plant Cell and Environment* **9**: 535-545.

Clement CR, Hopper MJ, Jones LHP. 1978. The uptake of nitrate by *Lolium perenne* from flowing culture solution. I. Effect of NO_3^- concentration. *Journal of Experimental Botany* **29**: 453-464.

Cohen SA, Michaud DP. 1993. Synthesis of a fluorescent derivatizing reagent, 6-aminoquinolyl-n-hydroxysuccinimidyl carbamate, and its application for the analysis of hydrolysate amino acids via high-performance liquid chromatography. *Analytical Biochemistry* **211**: 279-287.

Cooper HD, Clarkson DT. 1989. Cycling of amino-nitrogen and other nutrients between shoots and roots in cereals--A possible mechanism for integrating shoot and root in the regulation of nutrient uptake. *Journal of Experimental Botany* **40**: 753-762.

Dhugga KS, Waines JG. 1989. Analysis of nitrogen accumulation and use in bread and durum-wheat. *Crop Science* **29**: 1232-1239.

FAO 2006. Fertilizer use by crop. *FAO Fertilizer and Plant Nutrition Bulletin*. Rome: Food and Agriculture Organisation of the United Nations. 108.

Filleur S, Dorbe MF, Cerezo M, Orsel M, Granier F, Gojon A, Daniel-Vedele F. 2001. An arabidopsis T-DNA mutant affected in Nrt2 genes is impaired in nitrate uptake. *FEBS Letters* **489**: 220-224.

Forde BG. 2002. Local and long-range signalling pathways regulating plant responses to nitrate. *Annual Reviews of Plant Biology* **53**.

Forde BG, Clarkson DT 1999. Nitrate and ammonium nutrition of plants: Physiological and molecular perspectives. *Advances in Botanical Research*, 1-90.

Garnett TP, Shabala SN, Smethurst PJ, Newman IA. 2003. Kinetics of ammonium and nitrate uptake by eucalypt roots and associated proton fluxes measured using ion selective microelectrodes. *Functional Plant Biology* **30**: 1165-1176.

Glass ADM. 2003. Nitrogen use efficiency of crop plants: physiological constraints upon nitrogen absorption. *Critical Reviews in Plant Sciences* **22**: 453-470.

Gojon A, Nacry P, Davidian JC. 2009. Root uptake regulation: a central process for NPS homeostasis in plants. *Current Opinion in Plant Biology* **12**: 328-338.

Good AG, Shrawat AK, Muench DG. 2004. Can less yield more? Is reducing nutrient input into the environment compatible with maintaining crop production? *Trends In Plant Science* **9**: 597-605.

Goyal SS, Huffaker RC. 1986. The uptake of NO_3^-, NO_2^-, and NH_4^+ by intact wheat (*Triticum aestivum*) seedlings. I. Induction and kinetics of transport systems. *Plant Physiology* **82**: 1051-1056.

Guo FQ, Wang R, Chen M, Crawford NM. 2001. The Arabidopsis dual-affinity nitrate transporter gene AtNRT1.1 (CHL1) is activated and functions in nascent organ development during vegetative and reproductive growth. *Plant Cell* **13**: 1761-1777.

584 **Henriksen GH, Spanswick RM. 1993.** Investigation of the apparent Induction of nitrate uptake in
585 barley (*Hordeum vulgare* L) Using NO_3^--selective microelectrodes - modulation coarse
586 regulation of NO_3^- uptake by exogenous application of downstream metabolites in the NO_3^-
587 assimilatory pathway. *Plant Physiology* **103**: 885-892.
588 **Ho CH, Lin SH, Hu HC, Tsay YF. 2009.** CHL1 functions as a nitrate sensor in plants. *Cell* **138**:
589 1184-1194.
590 **Hourcade DE, Bugg M, Loussaert DF 1986**. The use of Gaspe variety for the study of pollen and
591 anther development of maize (*Zea mays*).In Mulcahy DL, Mulcahy GB, Ottaviano E.
592 *Biotechnology and Ecology of Pollen*: Springer-Verlag, New York. 319-324.
593 **Huang NC, Liu KH, Lo HJ, Tsay YF. 1999.** Cloning and functional characterization of an
594 Arabidopsis nitrate transporter gene that encodes a constitutive component of low-affinity
595 uptake. *Plant Cell* **11**: 1381-1392.
596 **Imsande J, Touraine B. 1994.** N demand and the regulation of nitrate uptake. *Plant Physiology* **105**:
597 3-7.
598 **Jackson WA, Flesher D, Hageman RH. 1973.** Nitrate uptake by dark-grown corn seedlings. Some
599 characteristics of the apparent induction. *Plant Physiology* **51**: 120-127.
600 **Johnson CM, Stout PR, Brewer TC, Carlton AB. 1957.** Comparative chlorine requirements of
601 different plant species. *Plant and Soil* **8**: 337-353.
602 **Kronzucker HJ, Siddiqi MY, Glass ADM. 1995.** Kinetics of NO_3^- influx in spruce. *Plant*
603 *Physiology* **109**: 319-326.
604 **Lee RB. 1982.** Selectivity and kinetics of ion uptake by barley plants following nutrient deficiency.
605 *Annals of Botany* **50**: 429-449.
606 **Lee RB, Drew MC. 1986.** Nitrogen-13 studies of nitrate fluxes in barley roots. II. Effect of plant N-
607 status on the kinetic parameters of nitrate influx. *Journal of Experimental Botany* **37**: 1768-
608 1779.
609 **Lee RB, Rudge KA. 1986.** Effects of nitrogen deficiency on the absorbtion of nitrate and ammonium
610 by barley plants. *Annals of Botany* **57**: 471-486.
611 **Lejay L, Tillard P, Lepetit M, Olive F, Filleur S, Daniel-Vedele F, Gojon A. 1999.** Molecular and
612 functional regulation of two NO_3^- uptake systems by N- and C-status of Arabidopsis plants.
613 *Plant Journal* **18**: 509-519.
614 **Lemaire G, Salette J. 1984.** Relationship between growth and nitrogen uptake in a pure grass stand
615 .1. Environmental-effects. *Agronomie* **4**: 423-430.
616 **Liu JX, Chen FJ, Olokhnuud C, Glass ADM, Tong YP, Zhang FS, Mi GH. 2009.** Root size and
617 nitrogen-uptake activity in two maize (*Zea mays*) inbred lines differing in nitrogen-use
618 efficiency. *Journal of Plant Nutrition and Soil Science-Zeitschrift Fur Pflanzenernahrung*
619 *Und Bodenkunde* **172**: 230-236.
620 **Liu KH, Huang CY, Tsay YF. 1999.** CHL1 is a dual-affinity nitrate transporter of Arabidopsis
621 involved in multiple phases of nitrate uptake. *Plant Cell* **11**: 865-874.
622 **Malagoli P, Laine P, Le Deunff E, Rossato L, Ney B, Ourry A. 2004.** Modeling nitrogen uptake in
623 oilseed rape cv Capitol during a growth cycle using influx kinetics of root nitrate transport
624 systems and field experimental data. *Plant Physiology* **134**: 388-400.
625 **Miller AJ, Fan XR, Orsel M, Smith SJ, Wells DM. 2007.** Nitrate transport and signalling. *Journal*
626 *of Experimental Botany* **58**: 2297-2306.
627 **Miller AJ, Fan XR, Shen QR, Smith SJ. 2008.** Amino acids and nitrate as signals for the regulation
628 of nitrogen acquisition. *Journal of Experimental Botany* **59**: 111-119.
629 **Minotti PL, Williams DC, Jackson WA. 1969.** Nitrate uptake by wheat as influenced by ammonium
630 and other cations. *Crop Science* **9**: 9-14.
631 **Moll RH, Kamprath EJ, Jackson WA. 1982.** Analysis and interpretation of factors which contribute
632 to efficiency of nitrogen-utilization. *Agronomy Journal* **74**: 562-564.
633 **Morgan MA, Jackson WA. 1988.** Inward and outward movement of ammonium in root systems:
634 transient responses during recovery from nitrogen deprivation in presence of ammonium.
635 *Journal of Experimental Botany* **39**: 179-191.

Nazoa P, Vidmar JJ, Tranbarger TJ, Mouline K, Damiani I, Tillard P, Zhuo DG, Glass ADM, Touraine B. 2003. Regulation of the nitrate transporter gene AtNRT2.1 in *Arabidopsis thaliana*: responses to nitrate, amino acids and developmental stage. *Plant Molecular Biology* **52**: 689-703.

Okamoto M, Kumar A, Li W, Wang Y, Siddiqi MY, Crawford NM, Glass ADM. 2006. High-affinity nitrate transport in roots of Arabidopsis depends on expression of the NAR2-like gene AtNRT3.1. *Plant Physiology* **140**: 1036-1046.

Okamoto M, Vidmar JJ, Glass ADM. 2003. Regulation of NRT1 and NRT2 gene families of *Arabidopsis thaliana*: Responses to nitrate provision. *Plant and Cell Physiology* **44**: 304-317.

Orsel M, Chopin F, Leleu O, Smith SJ, Krapp A, Daniel-Vedele F, Miller AJ. 2006. Characterization of a two-component high-affinity nitrate uptake system in Arabidopsis. Physiology and protein-protein interaction. *Plant Physiology* **142**: 1304-1317.

Peoples MB, Mosier AR, Freney JR 1995. Minimizing gaseous losses of nitrogen. In: Bacon PE ed. *Nitrogen fertilization in the environment*. New York: Marcel Dekker 505-602.

Plett D, Toubia J, Garnett T, Tester M, Kaiser BN, Baumann U. 2010. Dichotomy in the NRT Gene Families of Dicots and Grass Species. *PLOS One* **5**.

Rayment GE, Higginson FR. 1992. *Australian laboratory handbook of soil and water chemical methods*. Melbourne: Inkata.

Redinbaugh MG, Campbell WH. 1993. Glutamine synthetase and ferredoxin-dependent glutamate synthase expression in the maize (*Zea mays*) root primary response to nitrate (evidence for an organ-specific response). *Plant Physiology* **101**: 1249-1255.

Remans T, Nacry P, Pervent M, Girin T, Tillard P, Lepetit M, Gojon A. 2006. A central role for the nitrate transporter NRT2.1 in the integrated morphological and physiological responses of the root system to nitrogen limitation in Arabidopsis. *Plant Physiology* **140**: 909-921.

Reuter DJ, Robinson JB. 1997. *Plant Analysis: An Interpretation Manual*. Melbourne: CSIRO.

Santi S, Locci G, Monte R, Pinton R, Varanini Z. 2003. Induction of nitrate uptake in maize roots: expression of a putative high-affinity nitrate transporter and plasma membrane H^+-ATPase isoforms. *Journal of Experimental Botany* **54**: 1851-1864.

Siddiqi MY, Glass ADM, Ruth TJ, Fernando M. 1989. Studies of the regulation of nitrate influx by barley seedlings using 13-NO_3^-. *Plant Physiology* **90**: 806-813.

Siddiqi MY, Glass ADM, Ruth TJ, Rufty TW. 1990. Studies on the uptake of nitrate in barley. 1. Kinetics of $^{13}NO_3^-$ influx. *Plant Physiology* **93**: 1426-1432.

Sylvester-Bradley R, Kindred DR. 2009. Analysing nitrogen responses of cereals to prioritize routes to the improvement of nitrogen use efficiency. *Journal of Experimental Botany* **60**: 1939-1951.

Tsay Y-F, Chiu C-C, Tsai C-B, Ho C-H, Hsu P-K. 2007. Nitrate transporters and peptide transporters. *FEBS Letters* **581**: 2290-2300.

Vandesompele J, De Preter K, Pattyn F, Poppe B, Van Roy N, De Paepe A, Speleman F. 2002. Accurate normalization of real-time quantitative RT-PCR data by geometric averaging of multiple internal control genes. *Genome Biology* **3**.

Wirth J, Chopin F, Santoni V, Viennois G, Tillard P, Krapp A, Lejay L, Daniel-Vedele F, Gojon A. 2007. Regulation of root nitrate uptake at the NRT2.1 protein level in *Arabidopsis thaliana*. *Journal of Biological Chemistry* **282**: 23541-23552.

Wolt JD. 1994. *Soil solution chemistry: applications to environmental science and agriculture*. New York: Wiley.

Yong ZH, Kotur Z, Glass ADM. 2010. Characterization of an intact two-component high-affinity nitrate transporter from Arabidopsis roots. *Plant Journal* **63**: 739-748.

Zhuo DG, Okamoto M, Vidmar JJ, Glass ADM. 1999. Regulation of a putative high-affinity nitrate transporter (Nrt2;1At) in roots of *Arabidopsis thaliana*. *Plant Journal* **17**: 563-568.

687 **FIGURE LEGENDS**

688 **Figure 1.** Growth parameters across the dwarf maize (*Zea mays*) Gaspe Flint lifecycle of
689 plants grown at either 0.5 mM or 2.5 mM NO_3^-. (a) Shoot dry weight (DW). (b) Root DW. (c)
690 DW root: shoot ratio. (d) Shoot nitrogen concentration (mmoles gDW^{-1}). Fitted curves are as
691 described in the text. There was no significant difference between treatments for shoot
692 biomass, root biomass or root:shoot so there is just one fit to the pooled data. Values are
693 mean ± SEM (n=8 except for (d) where n=4), * indicates those points that are significantly
694 different between the two growth conditions ($p < 0.05$).

695 **Figure 2**. Unidirectional NO_3^- influx into the roots of the dwarf maize (*Zea mays*) Gaspe
696 Flint throughout the lifecycle of plants grown at either 0.5 mM or 2.5 mM NO_3^-. Nitrate
697 influx was measured using ^{15}N labelled NO_3^- over a 10-minute influx period with either (a) 50
698 µM NO_3^- or (b) 250 µM NO_3^-. Values are means ± SEM (n=4), * indicates those points that
699 are significantly different between the two growth conditions ($p < 0.05$).

700 **Figure 3**. Dwarf maize (*Zea mays*) Gaspe Flint whole plant net nitrogen uptake per gram root
701 dry weight as function of time. Net uptake was calculated from the fitted curves for shoot
702 DW, root DW and shoot N as shown in Fig. 1 and detailed in the text. Net nitrogen uptake is
703 compared to the experimentally determined nitrate flux capacity at 50 µM for different
704 nitrogen treatments (0.5 mM, open squares; 2.5 mM, filled squares; values are means ± SEM
705 (n=4)).

706 **Figure 4**. Unidirectional NO_3^- influx into the roots of dwarf maize (*Zea mays*) Gaspe Flint
707 plants grown at either 0.5 mM or 2.5 mM NO_3^- and moved to (a) higher or (b) lower NO_3^-
708 concentration at either day 15 or day 22 post emergence. Nitrate influx was measured using

709 ^{15}N labelled NO_3^- over a 10-minute influx period with 50 µM NO_3^-. Values are means ± SEM
710 (n=4). Dashed lines without symbols are the fluxes presented in Figure 2a.

711 **Figure 5**. Root transcript levels of various putative high and low affinity (NRT1, NRT2 and
712 NRT3) NO_3^- transporters throughout the lifecycle of dwarf maize (*Zea mays*) Gaspe Flint.
713 Plants were grown in nutrient solution containing either 0.5 mM (open squares) or 2.5 mM
714 (closed squares) NO_3^-. The broken lines correspond to maximum NO_3^- uptake capacity as
715 shown by the ^{15}N unidirectional flux analysis (see Fig. 2). Each data point is normalised
716 against control genes as described in the text. Values are means ± SEM (n=4), * indicates
717 those points that are significantly different between the two growth conditions ($p < 0.05$).
718 **Figure 6**. Transcript levels of various putative high and low affinity (NRT1, NRT2 and
719 NRT3) NO_3^- transporters in roots of dwarf maize (*Zea mays*) Gaspe Flint plants grown at
720 either 0.5 mM or 2.5 mM NO_3^- and moved to increased (upper panel) or decreased (lower
721 panel) NO_3^-concentration at either day 15 or day 22 post emergence. Each data point is
722 normalised against control genes as described in the text. Values are means ± SEM (n=4).
723 Values are means ± SEM (n=4). Dashed lines without symbols are the transcript values of
724 plants maintained with constant nitrate as presented in Figure 4.

725 **Figure 7**. Nitrate concentration in youngest collared leaf (a) and root (b) tissue of dwarf
726 maize (*Zea mays*) Gaspe Flint plants grown at either 0.5 mM or 2.5 mM NO_3^-. The broken
727 lines correspond to maximum NO_3^- uptake capacity as shown by the ^{15}N unidirectional flux
728 analysis (see Fig. 2). Values are means ± SEM (n=4), * indicates those points that are
729 significantly different between the two growth conditions ($p < 0.05$).

730 **Figure 8**. Total free amino acid concentration in root (a) and youngest collared leaf (b) tissue
731 of dwarf maize (*Zea mays*) Gaspe Flint plants grown at either 0.5 mM or 2.5 mM NO_3^-. The

broken lines correspond to maximum NO_3^- uptake capacity as shown by the ^{15}N unidirectional flux analysis (see Fig. 2). Values are means ± SEM (n=4), * indicates those points that are significantly different between the two growth conditions ($p < 0.05$).

Figure 9. Predicted ZmNRT2.1/2.2 protein levels based on a protein lifespan of 5 days and estimated as the sum of *ZmNRT2.1* and *ZmNRT2.2* transcripts at day x and those of the 4 previous days, in dwarf maize (*Zea mays*) Gaspe Flint plants plants grown at either (a) 0.5 mM or (b) 2.5 mM NO_3^-. Transcript levels are the summed *ZmNRT2.1* and *ZmNRT2.2* transcripts that were presented individually in Figure 4(a) whilst flux capacity is as presented in Figure 2(a). Panel (b) includes the flux capacity for plants grown at 0.5 mM NO_3^- but then moved to 2.5 mM nitrate at day 15 as presented in Figure 4(b).

SUPPORTING INFORMATION

Supporting information Table S1. Q-PCR primers for assay of maize gene expression are listed along with the Q-PCR product size (bp).

Supporting Information Table S2. Collection of fitting functions and associated parameters used in the modelling of shoot and root growth and shoot nitrogen content.

Supporting information Figure S1. Root and shoot dry weights of Gaspe Flint plants grown in hydroponics for 3 weeks at a range of NO_3^- concentrations.

Supporting information Figure S2. Growth of Gaspe Flint plants across the lifecycle.

Supporting information Figure S3. Functions used to fit biomass data.

Supporting information Figure S4. Unidirectional NO_3^- LATS flux and HATS flux measured on Gaspe Flint maize plants.

Supporting information Figure S5. Root transcript levels of various putative low affinity (NRT1 and NRT3) NO_3^- transporters throughout the lifecycle of Gaspe Flint.

Supporting information Figure S6. Transcript levels of various putative high and low affinity NO_3^- transporters in roots of Gaspe Flint plants exposed to changing N levels.

Supporting information Figure S7. Predicted ZmNRT2.1 protein levels .

Supporting Information Table S1. Q-PCR primers for assay of maize gene expression are listed along with the Q-PCR product size (bp).

Gene	Gene ID	Forward Primer(5'->3')	Reverse Primer (5'->3')	Q-PCR Product size (bp)
ZmNRT1.1A	GRMZM2G086496	CCTCCAGCAAGAAGAGCAAG	GACACCGAGAAGGTGGTCA	238
ZmNRT1.1B	GRMZM2G161459	GTCATCAGCGCCATCAACCT	GGGTCACACCGTGTGCCAAA	282
ZmNRT1.1C[a]	GMRZM2G112154	ACCCACGCCCAACTCTCC	GCCATGACTGAATGTTCCTTCTC	115
		TCGCCGCCTGGAGTAAGC	GCAGCGTGGTCAAGCAATC	148
ZmNRT1.1D	GMRZM2G161483	CAGCACCGCCATCGTCAG	GCCAGCAGCCAATAGAACTTG	114
ZmNRT1.2	GRMZM2G137421	GGTGCTGCCCATCTTCTTGT	ATGATGTGGTCGTAGACGGG	186
ZmNRT1.3	GMRZM2G176253	CGCCGTCTTCGTCGTCTTC	AAGTCGTCCATCTCCTTGTGC	102
ZmNRT1.4A	GMRZM2G064091	TGCTTGTGTTGTGTTGTGTTCTC	CTTCTTCCCGTCCATTGGTTTG	76
ZmNRT1.4B	GMRZM2G476069	GATTCCTTGCCGACTCCTTCC	GCTGCCTCACCTCTGTAGAC	211[b]
ZmNRT1.5A	GRMZM2G044851	CGTATGTTGTTCTTGTCTTCTTG	GTGCTATCGTCGTCAATGG	104
ZmNRT1.5B	GMRZM2G061303	GCCAACAGCATCAGCAAGTG	CGAGCGACAGGACCACCAG	145
ZmNRT2.1	GRMZM2G010280	CGACGAGAAGAGCAAGGGACT	GGCATATTCGTACATACAAAGAGGT	183
ZmNRT2.2	GRMZM2G010251	CGACGAGAAGAGCAAGGGACT	AGGTGAACATGGATGATGGAT	166
ZmNRT2.3	GRMZM2G163866	AGGAAGGGCATCGAGAACAT	CTTGCGCTGTGACGGCCTAC	179
ZmNRT2.5	GMRZM2G455124	GCATCGTCCCGTTCGTCTC	CCGTCTCCGTCTTGTACTTGG	129
ZmNRT3.1A	GRMZM2G179294	GCATCCACGCCTCTCTCAAG	TCAGCAACGACAGCCACTCAT	177
ZmNRT3.1B	GMRZM2G163494	CACCTCGTCACACACCACAG	CCAGCAGCAGCGGCAAAG	86
ZmNRT3.2	GMRZM2G808737	GTCGCTCATTCCTCGGTGTC	TTGATGTTGCCTTGTTCGTTCC	96
ZmGaPDh	GRMZM2G077927	GACAGCAGGTCGAGCATCTTC	GTCGACGACGCGGTTGCTGTA	114
ZmActin	GRMZM2G126069	CCAATTCCTGAAGATGAGTCT	TGGTAGCCAACCAAAAACAGT	156
ZmTubulin	GRMZM2G152466	GAGGACGGCGACGAGGGTGAC	CAAAGCGGGGGAATAAAGTCT	186
ZmElF1	GRMZM2G154218	GCCGCCAAGAAGAAATGATGC	CGCCAAAAGGAGAAATACAAG	220

[a] Amplification of a *ZmNRT1.1C* PCR product was attempted using two sets of Q-PCR primers and neither set amplified a product from cDNA. The gene appears to not be expressed in Gaspe roots as both sets amplified strong PCR products from gDNA.

[b] Gaspe Q-PCR product is longer than the predicted B73 product (108 bp) as the 2nd intron appears to not be spliced out of *ZmNRT1.4B* transcripts in Gaspe roots.

Supporting Information Table S2. Collection of fitting functions and associated parameters used in the modelling of shoot and root growth and shoot nitrogen content.

Quantity	Fit function	Parameter
Shoot dry weight (g)	$DW_{\mathrm{S}} = \frac{S_0 \exp(\mu_s t)}{1 + k \exp(-\nu_s t)}$	$k = 57.5$; $S_0 = 0.146$ gDW; $\mu_s = 0.0775$ d^{-1}; $\nu_s = 0.350$ d^{-1};
Root dry weight (g)	$DW_{\mathrm{R}} = R_0 \exp(\mu_r t)$	$R_0 = 0.0318$ gDW; $\mu_r = 0.0605$ d^{-1};
Shoot N content (%DW)	$N_{\mathrm{S}} = \frac{\alpha}{\gamma + (\mathrm{DW}_S)^{\beta}}$	$\alpha = 47.0$ wt%; $\beta = 1.22$; $\gamma = 9.05$; at 0.5 mM $\alpha = 27.1$ wt%; $\beta = 0.87$; $\gamma = 4.44$; at 2.5 mM
Root N content (%DW)	$N_{\mathrm{R}} = \delta$	$\delta = 3.68$ wt%; at 0.5 mM $\delta = 4.31$ wt%; at 2.5 mM

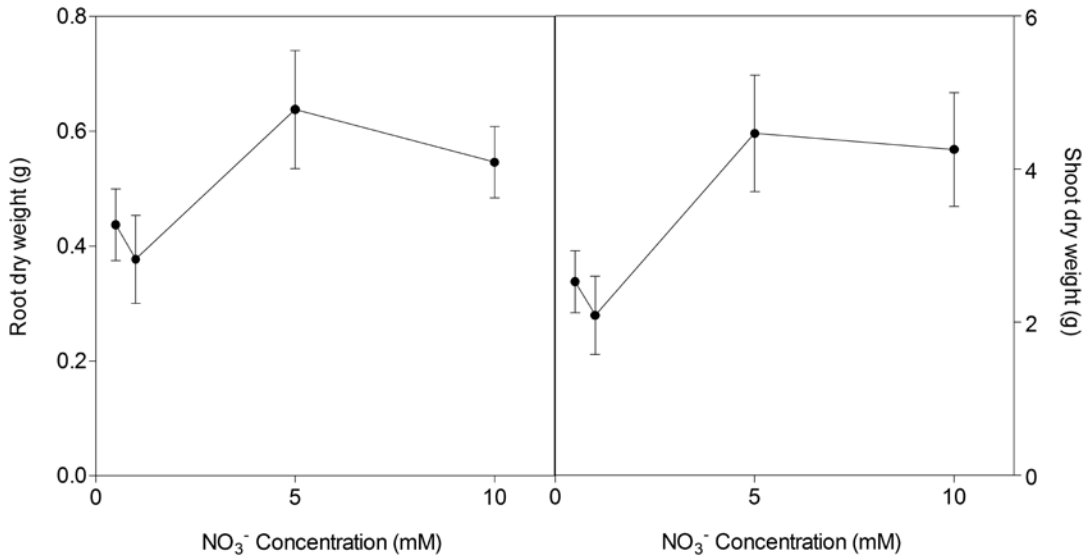

Supporting Information Figure S1. Root and shoot dry weights of Gaspe Flint plants grown in hydroponics for 3 weeks at a range of NO_3^- concentrations. Values are means ± SEM (n=6).

Day 14

Day 17

Day 25

Day 31

Day 34

Supporting Information Figure S2. Growth of Gaspe Flint harvest across the lifecycle. Images are of roots and shoots following removal of the root.

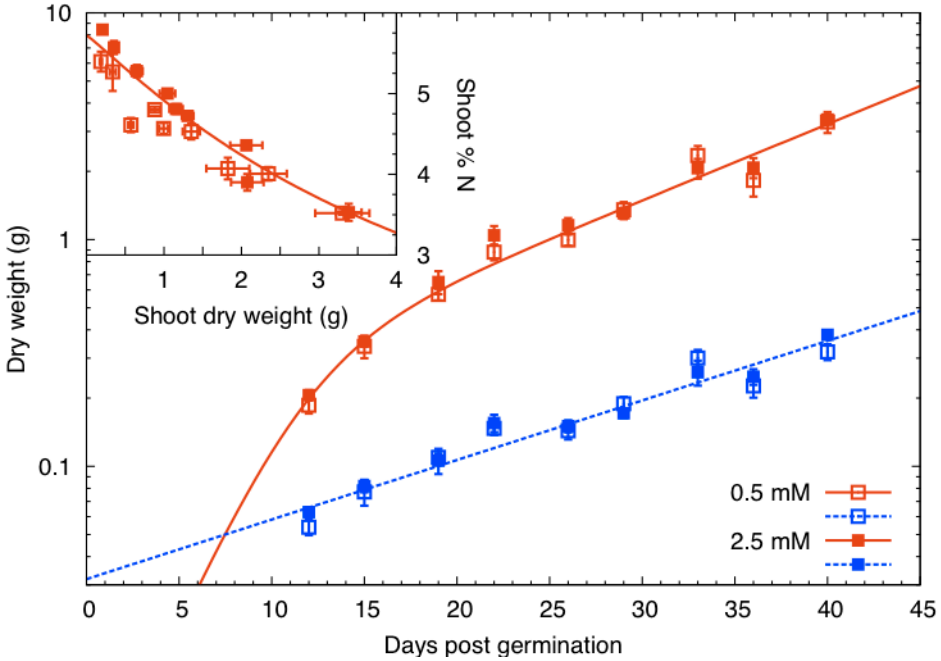

Supporting Information Figure S3. Functions used to fit biomass data. Root dry weight (dashed line) and shoot dry weight (solid line) as function of time for different nitrate treatments (0.5 mM, open squares; 2.5 mM, filled squares). Inset, shoot % N as a function of shoot dry weight. In both plots the lines represent fits to the data. Parameters for these fits can be found in the Supporting Information Table S2.

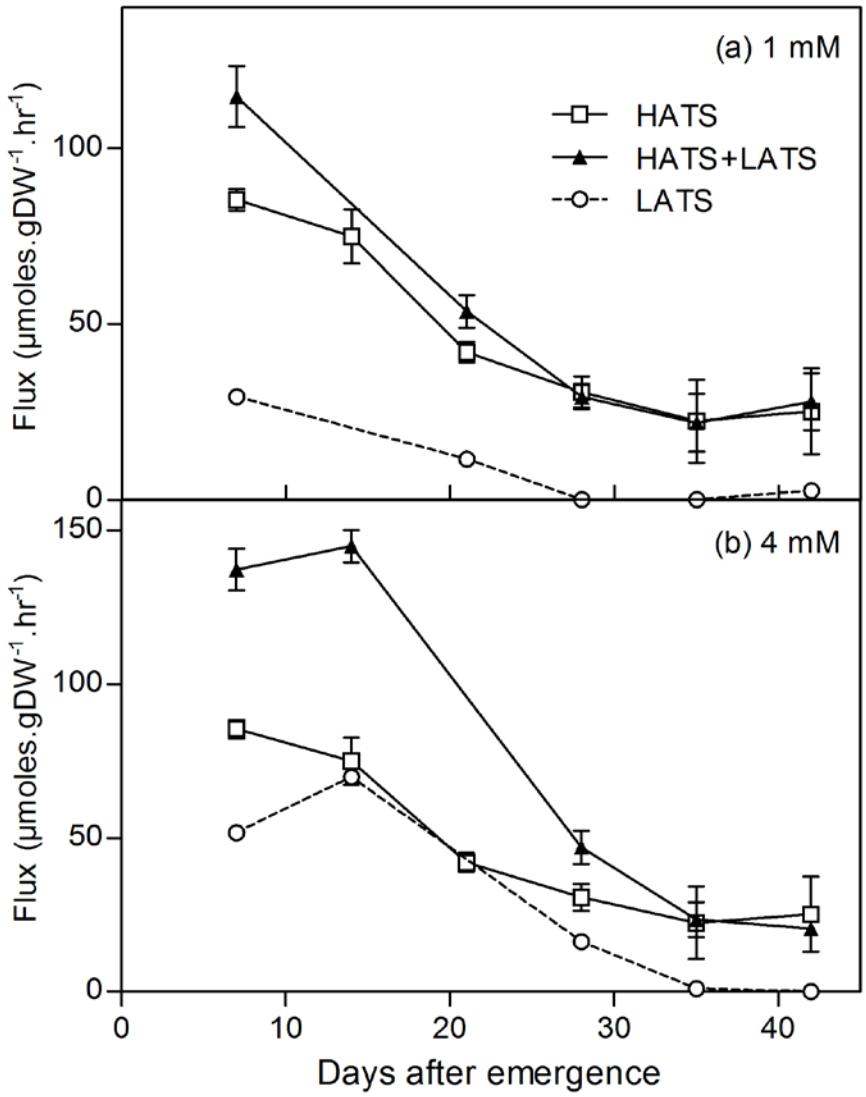

Supporting information Figure S4. Unidirectional NO_3^- LATS flux (1 and 4 mM NO_3^-) and HATS flux (250 µM NO_3^-) were measured on Gaspe Flint maize plants grown on adequate NO_3^- (5 mM NO_3^-). HATS uptake capacity was estimated as the average of the influx measured at 150 and 250 µM NO_3^-. HATS plus LATS uptake capacity was measured at both 1 mM and 4 mM NO_3^-. The LATS uptake capacity was estimated by subtracting the HATS uptake capacity from the HATS plus LATS uptake (as per Okamoto et al., 2003)**.** As in the results presented in Fig. 2, HATS activity remained high early in the vegetative growth period followed by a general decline across the developmental life cycle. LATS activity mirrored these trends albeit at a significantly lower capacity in the early growth phase (0-20 DAE) where it was 30% of the HATS at 1 mM NO_3^-. In contrast, at 4 mM NO_3^-, LATS activity was similar to HATS activity during early on but dropped from 20 DAE onwards.

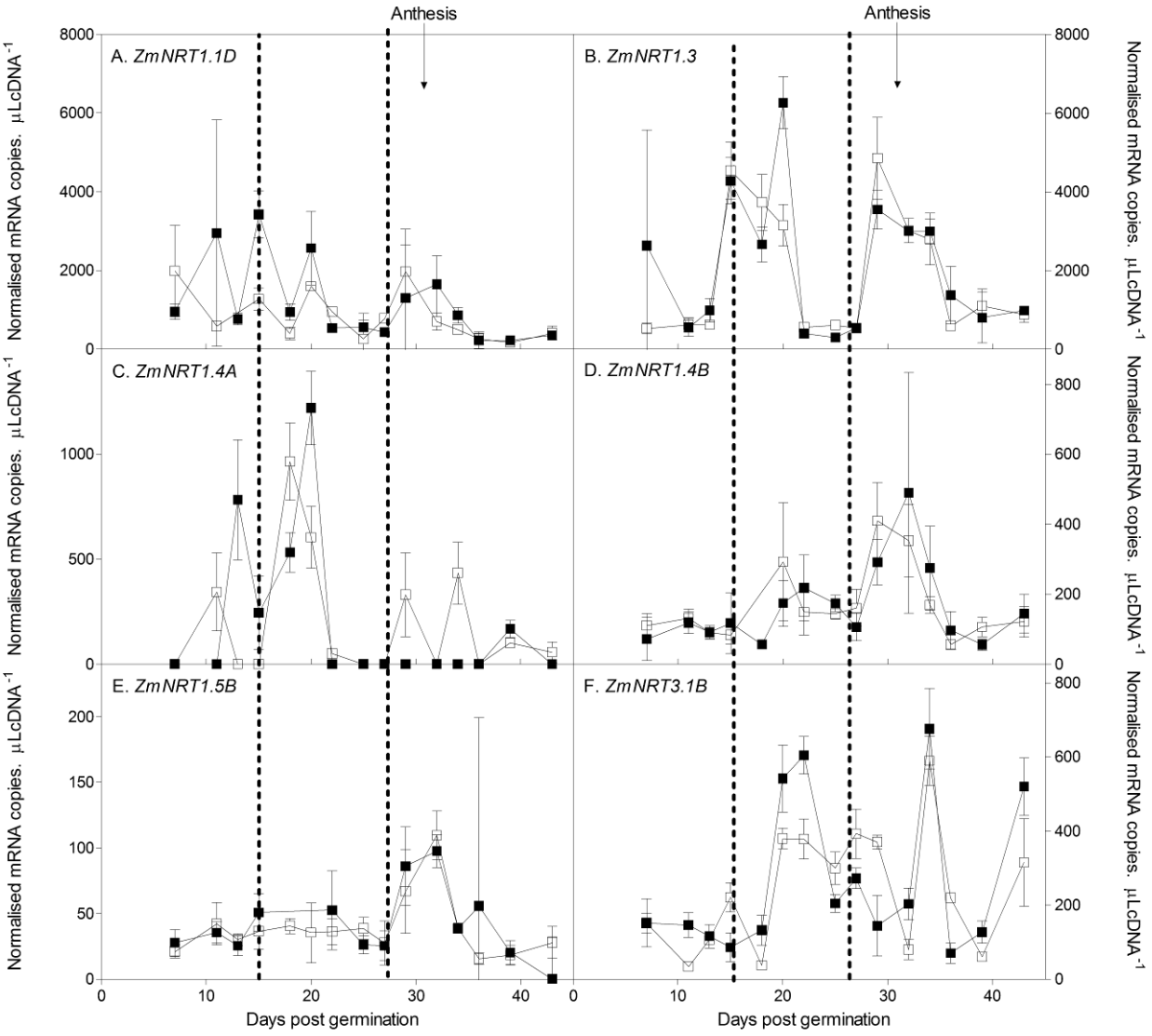

Supporting Information Figure S5. Root transcript levels of various putative high and low affinity (NRT1 and NRT3) NO_3^- transporters throughout the lifecycle of Gaspe Flint. Plants were grown in nutrient solution containing either 0.5 mM (open squares) or 2.5 mM (closed squares) NO_3^-. The broken lines correspond to maximum NO_3^- uptake capacity as shown by the ^{15}N unidirectional flux analysis (see Fig. 2). Each data point is normalised against control genes as described in the text. Values are means ± SEM (n=4).

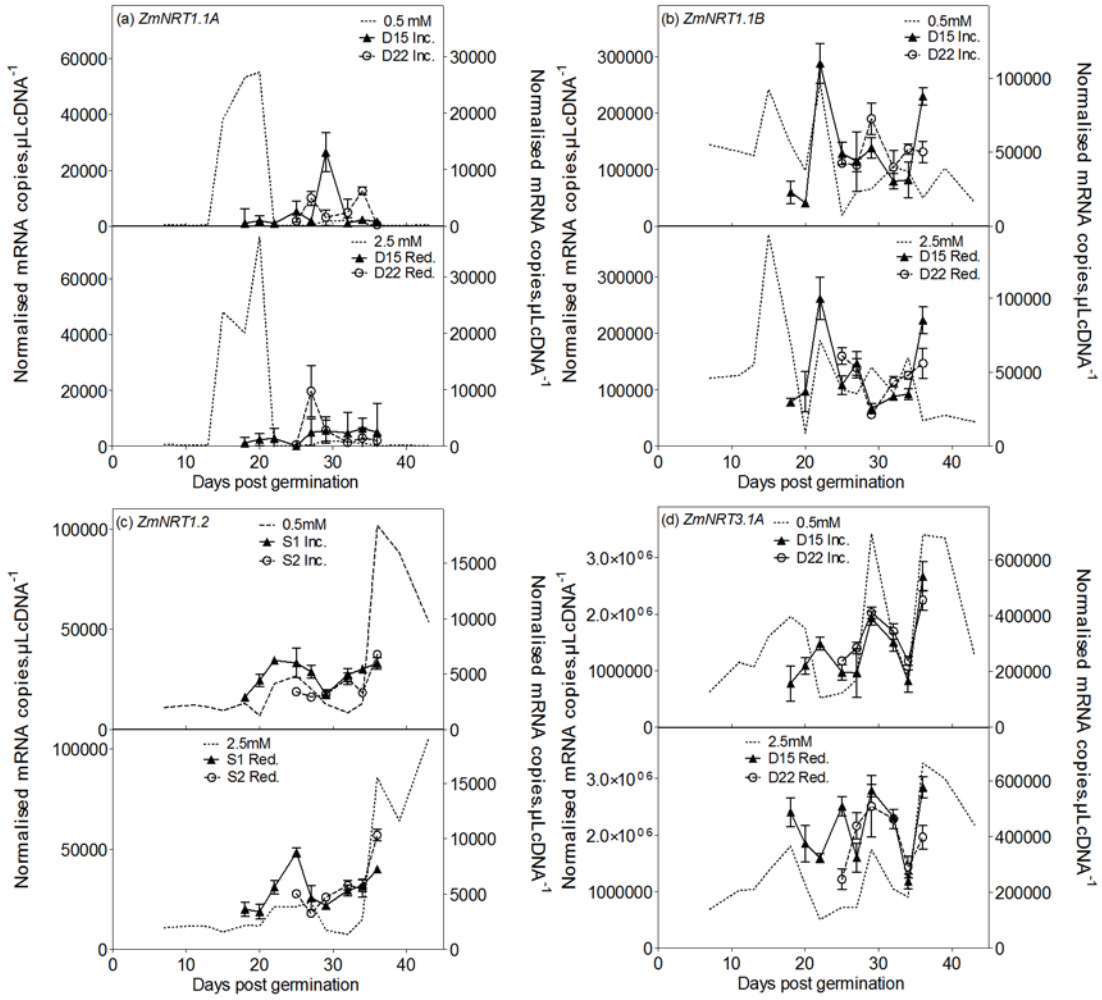

Supporting information Figure S6. Transcript levels of various putative high and low affinity (NRT1, NRT2 and NRT3) NO_3^- transporters in roots of Gaspe Flint plants grown at either 0.5 mM or 2.5 mM NO_3^- and moved to increased (upper panel) or decreased (lower panel) NO_3^-concentration at either day 15 or day 22 post emergence. Each data point is normalised against control genes as described in the text. Values are means ± SEM (n=4). Values are means ± SEM (n=4). Dashed lines without symbols are the transcript values of plants maintained with constant nitrate as presented in Figure 4.

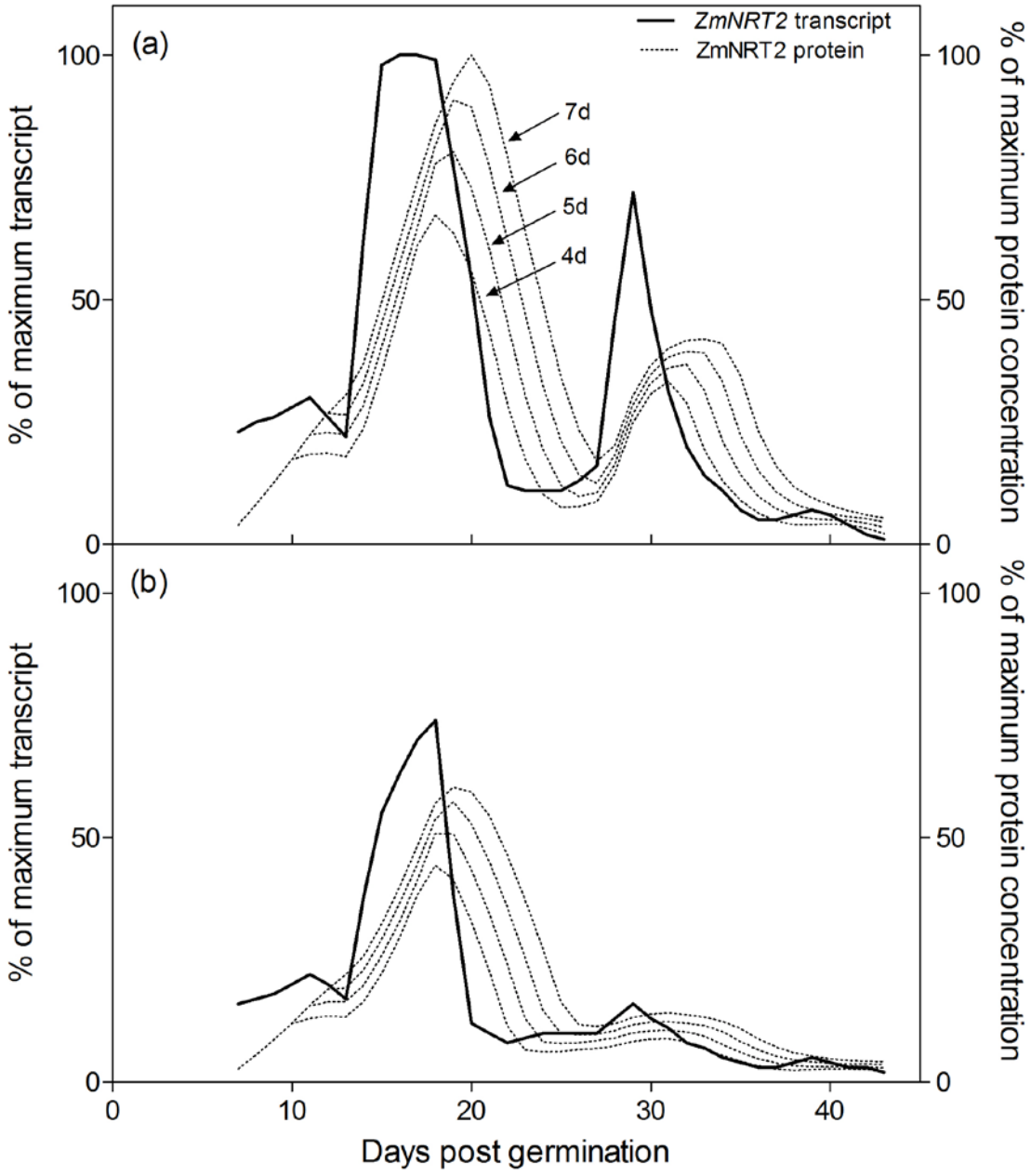

Supporting information Figure S7. Predicted ZmNRT2.1/2.2 protein levels (dotted lines) based on a protein lifespan estimated as the sum of *ZmNRT2.1* and *ZmNRT2.2* transcripts at day x and those of the previous 4-7 days, in plants grown at either (a) 0.5 mM or (b) 2.5 mM NO_3^-. Transcript levels are the summed *ZmNRT2.1* and *ZmNRT2.2* transcripts that were presented individually in Figure 4(a) whilst flux capacity is as presented in Figure 2(a).

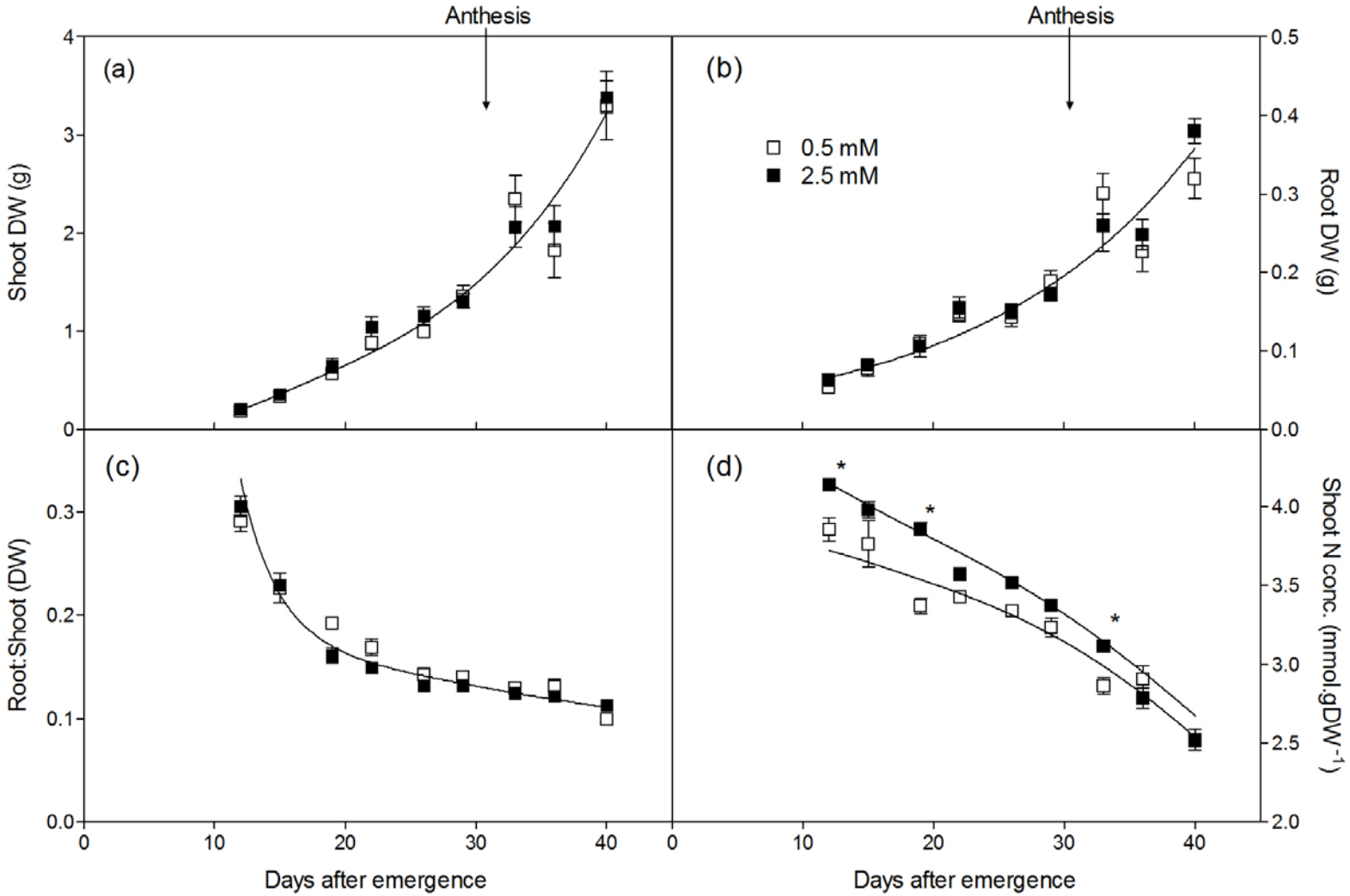

Figure 1. Growth parameters across the Gaspe Flint lifecycle of plants grown at either 0.5 mM or 2.5 mM NO_3^-. (a) Shoot dry weight (DW). (b) Root DW. (c) DW root: shoot ratio. (d) Shoot nitrogen concentration (mmoles.gDW^{-1}). Fitted curves are as described in the text. There was no significant difference between treatments for shoot biomass, root biomass or root:shoot so there is just one fit to the pooled data. Values are mean ± SEM (n=8 except for (d) where n=4), * indicates those points that are significantly different between the two growth conditions ($p < 0.05$).

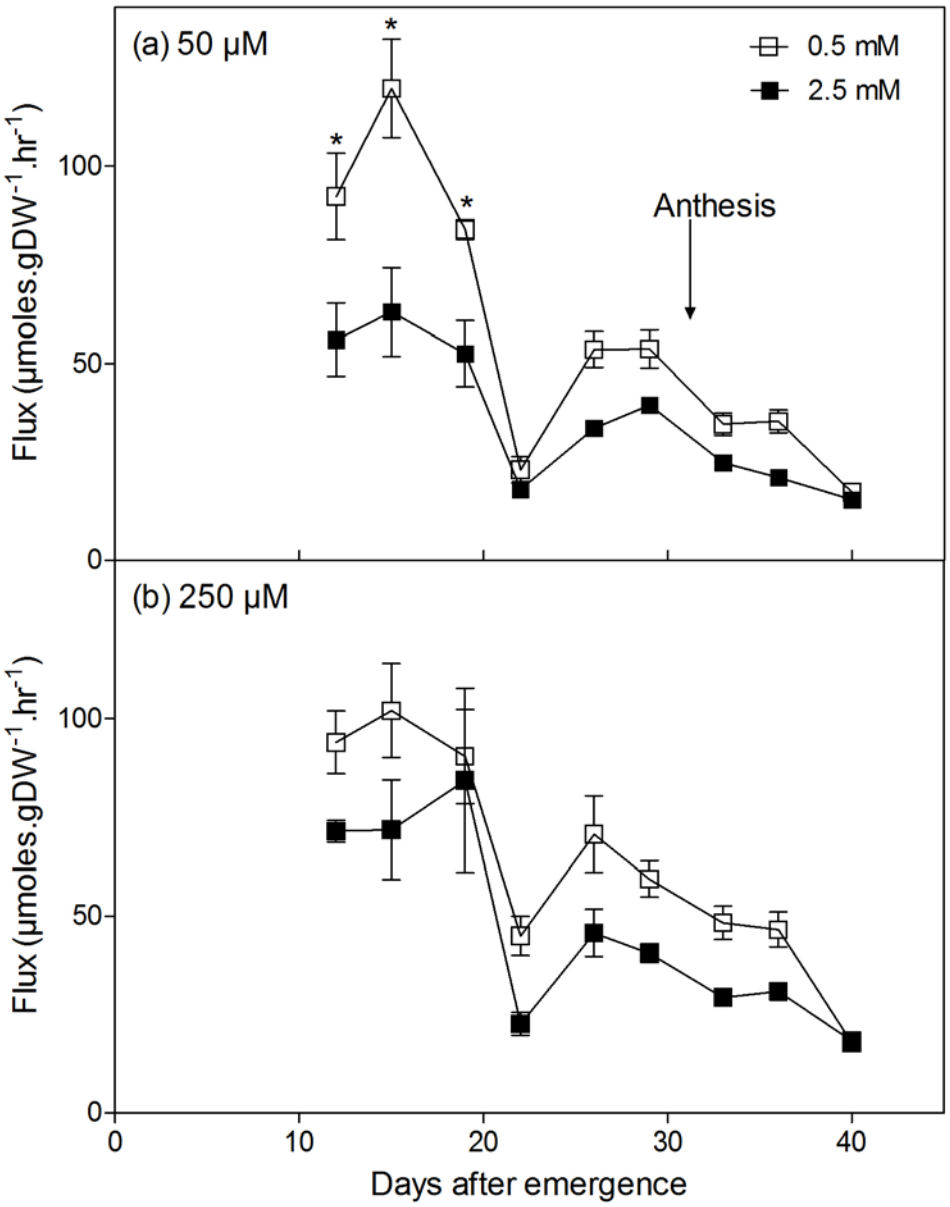

Figure 2. Unidirectional NO_3^- influx into the roots of Gaspe Flint throughout the lifecycle of plants grown at either 0.5 mM or 2.5 mM NO_3^-. Nitrate influx was measured using ^{15}N labelled NO_3^- over a 10-minute influx period with either (a) 50 µM NO_3^- or (b) 250 µM NO_3^-. Values are means ± SEM (n=4), * indicates those points that are significantly different between the two growth conditions ($p < 0.05$).

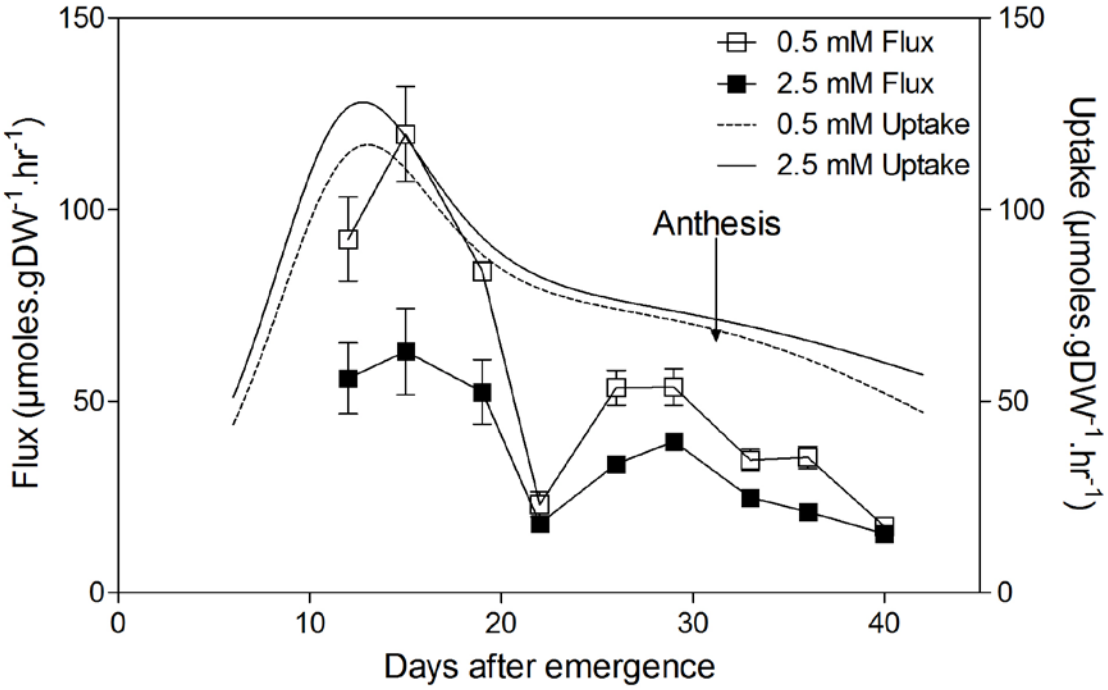

Figure 3. Whole plants net nitrogen uptake per gram root dry weight as function of time. Net uptake was calculated from the fitted curves for shoot DW, root DW and shoot %N as shown in Figure 1 and detailed in the text. Net nitrogen uptake is compared to the experimentally determined nitrate flux capacity at 50 µM for different nitrogen treatments (0.5 mM, open squares; 2.5 mM, filled squares).

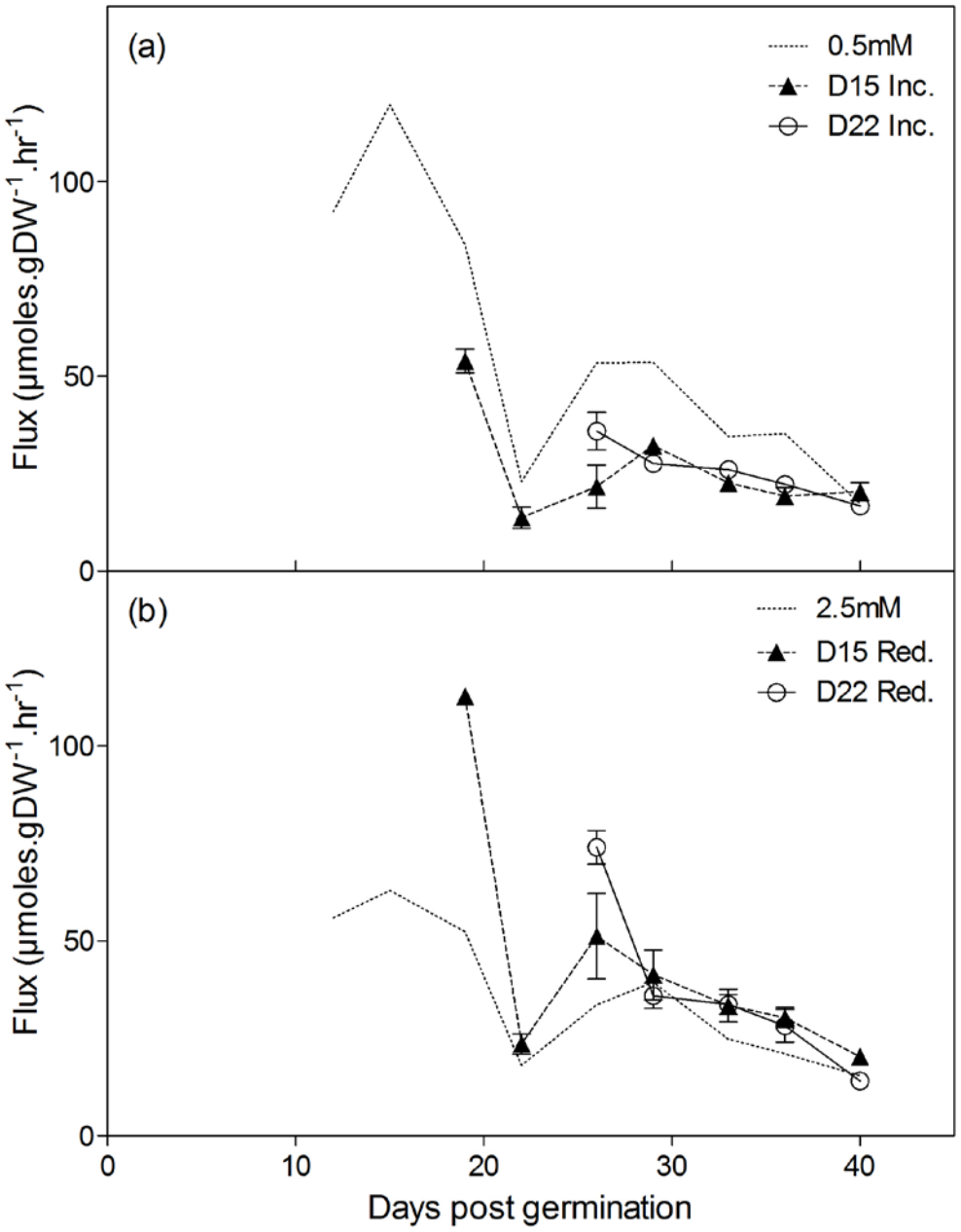

Figure 4. Unidirectional NO_3^- influx into the roots of Gaspe Flint plants grown at either 0.5 mM or 2.5 mM NO_3^- and moved to (A) higher or (B) lower NO_3^- concentration at either day 15 or day 22 post emergence. Nitrate influx was measured using ^{15}N labelled NO_3^- over a 10-minute influx period with 50 µM NO_3^-. Values are means ± SEM (n=4). Dashed lines without symbols are the fluxes presented in Figure 2A.

Figure 5. Root transcript levels of various putative high and low affinity (NRT1, NRT2 and NRT3) NO_3^- transporters throughout the lifecycle of Gaspe Flint. Plants were grown in nutrient solution containing either 0.5 mM (open squares) or 2.5 mM (closed squares) NO_3^-. The broken lines correspond to maximum NO_3^- uptake capacity as shown by the ^{15}N unidirectional flux analysis (see Fig. 2). Each data point is normalised against control genes as described in the text. Values are means ± SEM (n=4), * indicates those points that are significantly different between the two growth conditions ($p < 0.05$).

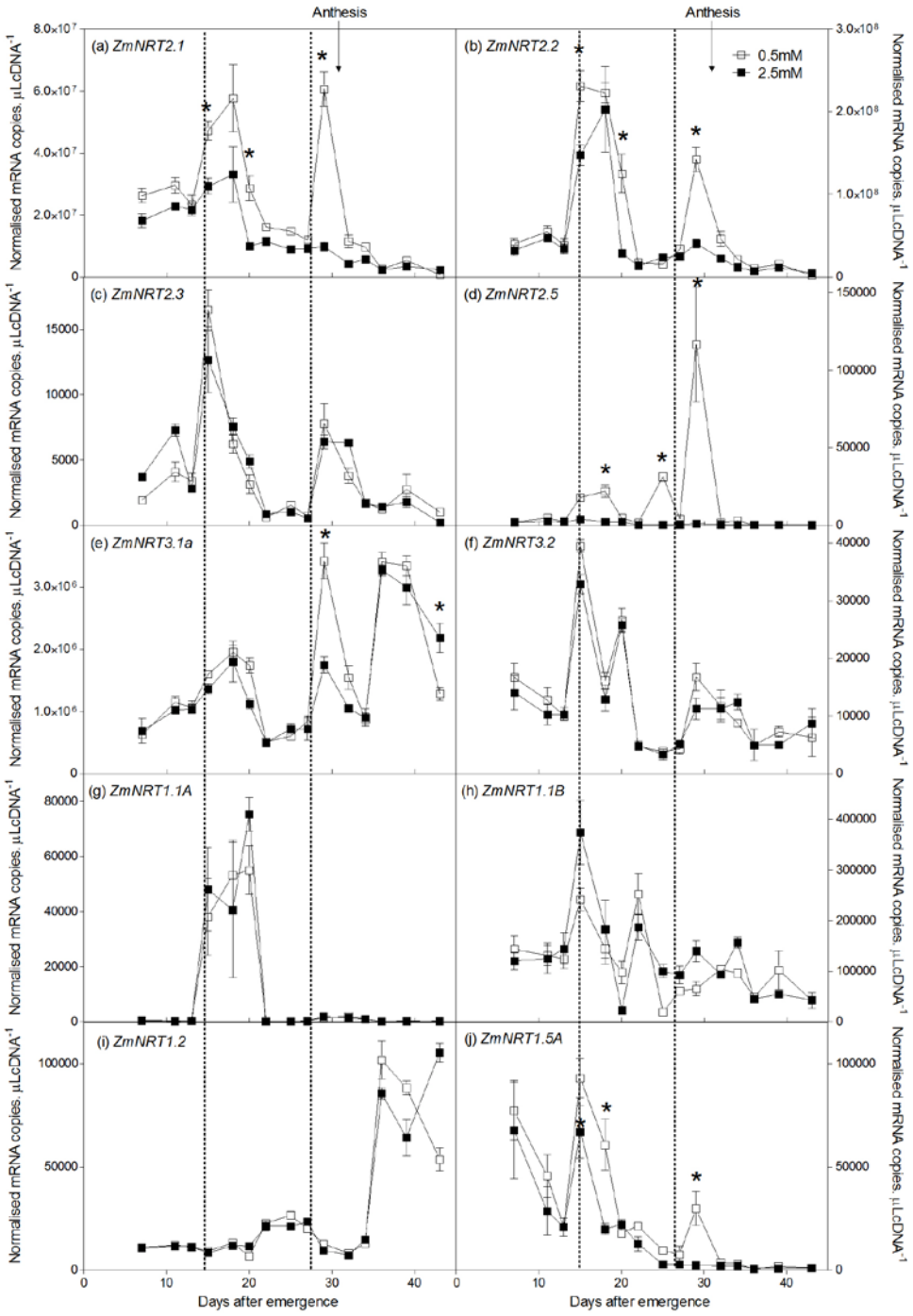

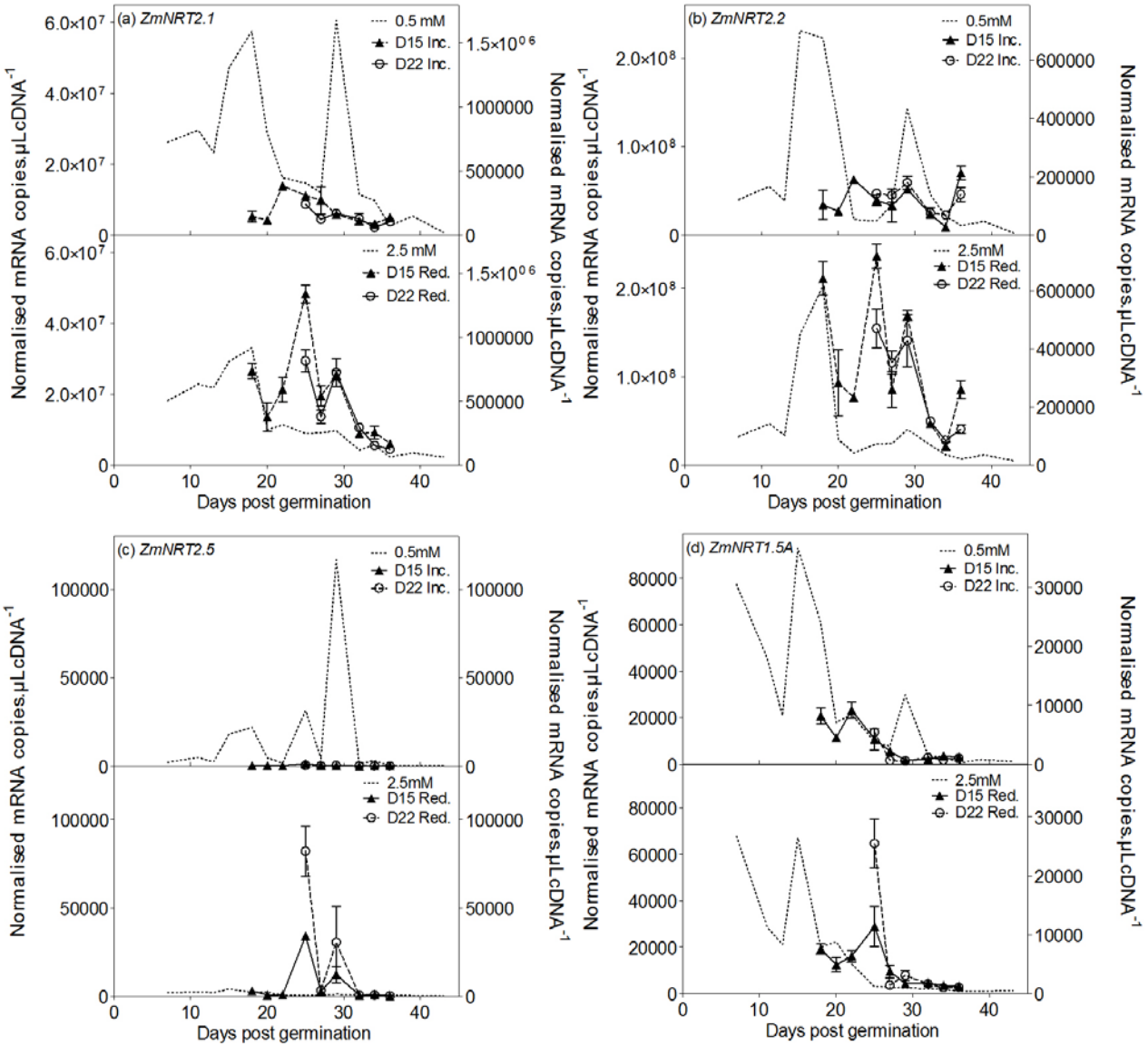

Figure 6. Transcript levels of various putative high and low affinity (NRT1, NRT2 and NRT3) NO_3^- transporters in roots of Gaspe Flint plants grown at either 0.5 mM or 2.5 mM NO_3^- and moved to increased (upper panel) or decreased (lower panel) NO_3^-concentration at either day 15 or day 22 post emergence. Each data point is normalised against control genes as described in the text. Values are means ± SEM (n=4). Values are means ± SEM (n=4). Dashed lines without symbols are the transcript values of plants maintained with constant nitrate as presented in Figure 5.

Figure 7. Nitrate concentration in youngest collared leaf **(A)** and root **(B)** tissue of Gaspe Flint plants grown at either 0.5 mM or 2.5 mM NO_3^-. The broken lines correspond to maximum NO_3^- uptake capacity as shown by the ^{15}N unidirectional flux analysis (see Figure 2). Values are means ± SEM (n=4), * indicates those points that are significantly different between the two growth conditions ($p < 0.05$).

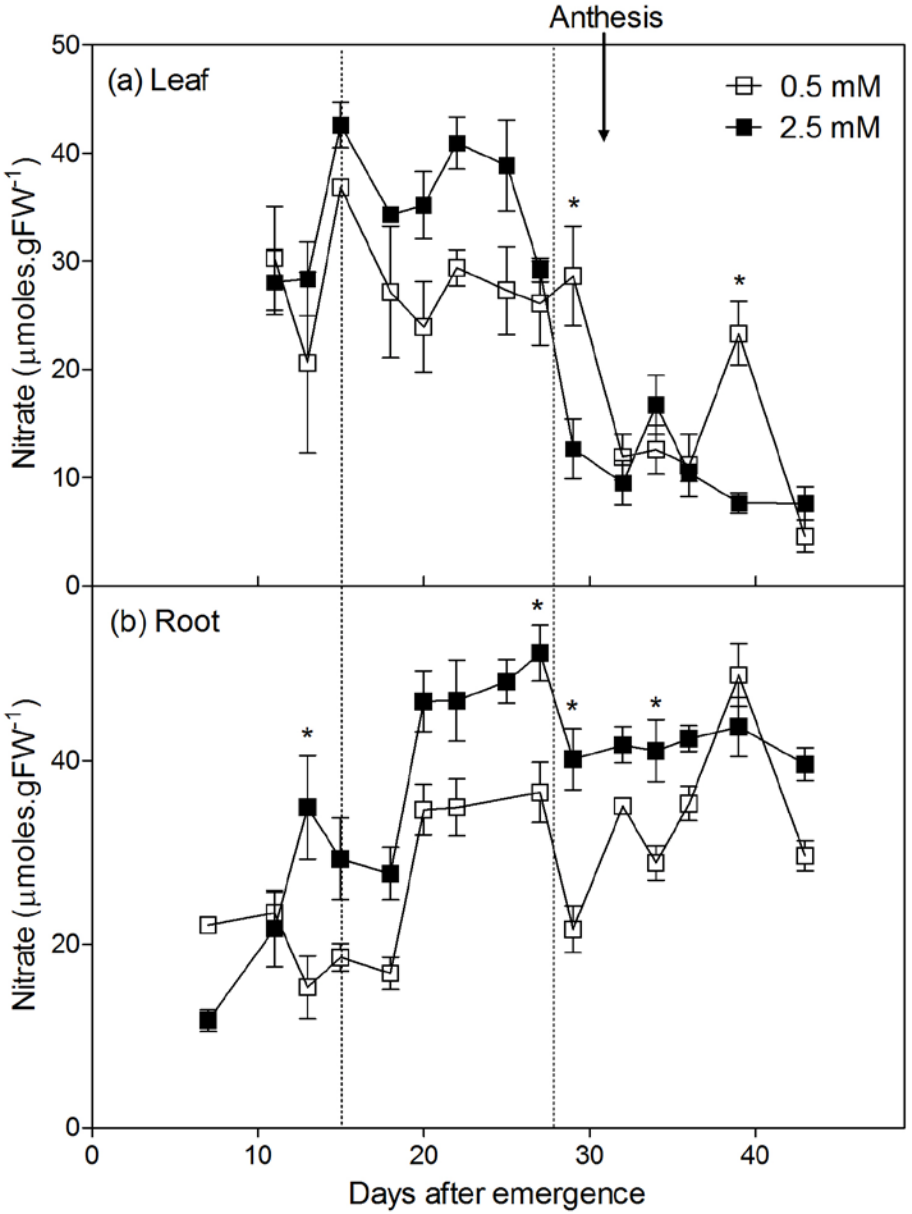

Figure 8. Total free amino acid concentration in root (a) and youngest collared leaf (b) tissue of Gaspe Flint plants grown at either 0.5 mM or 2.5 mM NO_3^-. The broken lines correspond to maximum NO_3^- uptake capacity as shown by the ^{15}N unidirectional flux analysis (see Fig. 2). Values are means ± SEM (n=4), * indicates those points that are significantly different between the two growth conditions ($p < 0.05$).

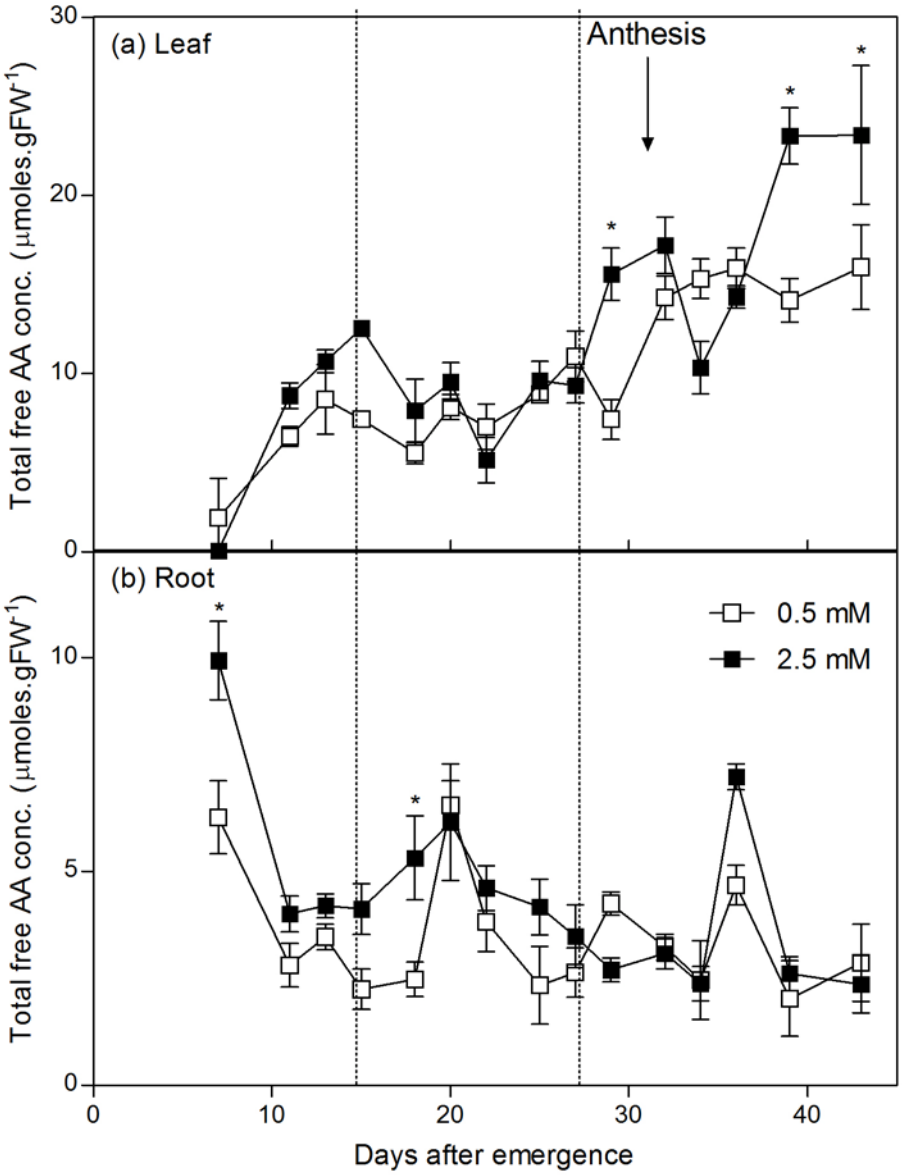

Figure 9. Predicted ZmNRT2.1/2.2 protein levels based on a protein lifespan of 5 days and estimated as the sum of *ZmNRT2.1* and *ZmNRT2.2* transcripts at day x and those of the 4 previous days, in plants grown at either (a) 0.5 mM or (b) 2.5 mM NO_3^-. Transcript levels are as presented in Figure 4(a) whilst flux capacity is as presented in Figure 2(a). Panel (b) includes the flux capacity for plants grown at 0.5 mM NO_3^- but then moved to 2.5 mM nitrate at day 15 as presented in Figure 4(b).